A report on the specifications of a reference signal processing architecture for a ROCOF instrument, including the uncertainty specification for each element of the measurement chain (including transducers, analogue signal processing, filtering, analogue to digital convertors, digital signal processing, computational processing).

Paul Wright (NPL, UK),
Martin Sira (CMI, CZ),
and Andrew Roscoe (University of Strathclyde, UK).

This work is part of a joint pre-normative research project “ROCOF” and has received funding from the EMPIR programme co-financed by the Participating States and the European Union’s Horizon 2020 research and innovation programme.

TABLE OF CONTENTS

1 Introduction and Aim

The purpose of this document is to propose a reference architecture for a ROCOF instrument. This reference implementation is intended as an aid to a manufacturer of a ROCOF instrument and is proposed as an informative to a ROCOF standard to demonstrate a method to implement a compliant instrument.

The architecture is intended to be as simple as possible for ROCOF and where appropriate, builds-on the existing IEEE C37.118.1 Annex C [1] heterodyne based example, such that existing hardware can be used to implement ROCOF. If desired, other experts can extend the reference model to cover implementations of PMUs and/or Power Quality instruments.

Other instrument architectures such as those based on phase locked loops and frequency estimators are not considered here.

The proposed reference model for a ROCOF instrument is divided into a sampling part (in hardware) and a processing part (in a processor, implemented by firmware and/or software).

The document will consider each component in turn, giving some commentary on the functionality, advice on implementation requirements, and an accuracy/uncertainty recommendation to assist manufacturers in the design of a ROCOF instrument. In some cases, an uncertainty analysis is calculated using Monte-Carlo simulations in order to assess the sensitivity of the final frequency and ROCOF results to errors in the components of the architecture. The details of the Monte-Carlo simulations is given in an Appendix.

The architecture for a heterodyne based instrument [1] is shown in Fig.1 and a summary of the components is given below.

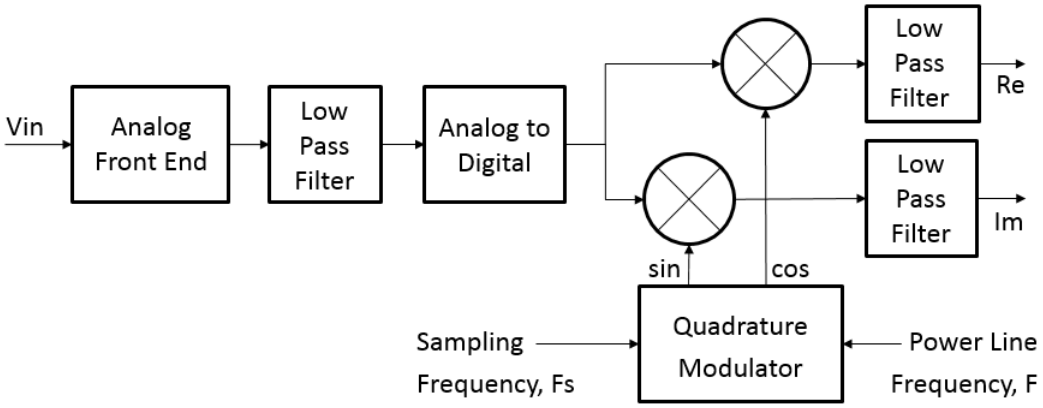

Fig. 1, one phase of a heterodyne based ROCOF instrument architecture.

1.1 Sampling Part

The sampling part of the ROCOF instrument contains electronic hardware as follows:

- A transducer to convert the supply system voltage to low signal levels suitable for the instruments electronics.
- An analogue front end, possibly containing buffer amplifier and over-voltage protection.
- A low pass “anti-aliasing” filter.
- An analogue to digital convertor (ADC).
- A sampling clock (not necessarily disciplined by GPS unless PMU operation is required).

The sampling clock will be common to all channels of a poly-phase instrument, the other components will be replicated for each channel of a poly-phase instrument.

1.2 Processing Part.

The processing part consists of:

- A real-time arithmetic processing engine.
- Communications and time stamping to dispatch the results to other systems.

And the following software/firmware real-time implantations:

- A quadrature oscillator.
- A heterodyne for each quadrature path.
- Digital filters.
- A positive sequence calculator.
- Phase and frequency differentiation.
- An output decimator.

2 Sampling Part; Details of Each Component.

A description, quality considerations and uncertainty recommendations are given for each hardware component in-turn.

2.1 Sampling Part Front End Signal to Noise Ratio (SNR)

Rather than discussing this issue for each component of the *Sampling Part*, the aggregate SNR is discussed here.

Front-end white noise is introduced by analogue instrumentation and ADC (Analogue to Digital Converter) quantisation effects. These introduce white or “nearly white” noise into the digital measurement process. These can result in an excessively noisy frequency measurement, and in the case of a ROCOF measurement the resulting magnitude is often swamped by noise. This is analysed in detail in [2].

The following equation (Eq. 1) can be used to translate between ENOB (the Effective Number of Bits) which is often quoted for ADCs and the SNR [3].

$$SNR_{dB} = 6.02 \cdot ENOB + 1.76 \quad \text{dB} \qquad \text{Eq. 1}$$

A sampling process with N bits will always have ENOB ≤ N, by a quantity dependent on the analogue noise and ADC imperfections. The ENOB may be further degraded in the final application due to analogue sensors, cables, circuits or amplifiers in the signal chain.

As many ADCs are not used to full-range in order to allow for the non-clipped digitisation of signal spikes, the SNR which is nomally quoted w.r.t. full scale is effectivly degraded. This can be accounted for as described in [3].

The effect of SNR on frequency and ROCOF measurements depends on the relative power spectral density of noise $L_{dBc}(f)$ which is constrained by the given sampling frequency (f_s) of the ADC, where:

$$L_{dBc}(f) = -SNR_{dB} - 10\log_{10}\left(\frac{f_s}{2}\right) \quad \text{dBc/Hz} \qquad \text{Eq. 2}$$

And the linear noise power density $(L(f))$ relative to a carrier with unity power is given by:

$$L(f) = 10^{\left(\frac{L_{dBc}(f)}{10}\right)} \qquad \text{Eq. 3}$$

Similarly,

$$SNR = 10^{\left(\frac{SNR_{dB}}{10}\right)} \qquad \text{Eq. 4}$$

Reference [1] also defines:

$$\sqrt{L(f)} = \sqrt{\frac{2}{SNR \cdot f_s}} \qquad \text{Eq. 5}$$

Reference [1] derives the following equations to give the frequency error (FE) and ROCOF error (RFE) related to the front end noise density $L(f)$.

$$FE_{3\phi RMS} \approx \sqrt{\frac{L(f)}{3}} \sqrt{\int_{f_N=0}^{\frac{f_S}{2}} \left| f_N H(f_N) \right|^2 \cdot df_N} \qquad \text{Eq. 6}$$

$$RFE_{3\phi RMS} \approx 2\pi \sqrt{\frac{L(f)}{3}} \sqrt{\int_{f_N=0}^{\frac{f_S}{2}} \left| f_N^2 H(f_N) \right|^2 \cdot df_N} \qquad \text{Eq. 7}$$

Where f_n is the noise component frequency over 0 to half the sampling frequency, $H(f_n)$ is the frequency response (transfer function) of the filters used in the ROCOF instrument.

In an application with SNR higher or lower than that presented, every 6 dB increase of SNR halves the Frequency Error (FE) and ROCOF Error (RFE) and vice versa. Section 2.7 shows plots of RFE change with SNR. The effect of sample rate also needs careful consideration, higher sampling rates will spread the noise over a wider Nyquist band lessening its effect at un-filtered frequencies.

Three-phase analysis allows a further SNR benefit of $1/\sqrt{3}$ (4.77dB) to be gained by averaging the 3 results.

2.2 Transducers

2.2.1 Description.

The transducer reduces the supply system voltage to low signal levels suitable for electronics. The nominal input (primary) levels to the transducers are defined by the supply system voltage. The output (secondary) signal levels are defined by the peak (not r.m.s.) working input voltage of the analogue electronics. Consideration should be given to the possibility of spikes on the supply system that could increase the secondary peaks that cause over-range and saturation in the electronics. The transducers should be able to safely withstand over voltages consistent with the fault level of the supply system.

2.2.2 Quality Considerations

Non-linearity's in the transducers will distort the output signal, however if the algorithm is designed to reject steady-state harmonic distortion with high attenuation this should not be a problem for ROCOF.

Delays (time constants) will cause absolute phase errors, giving rise to different angular errors at different harmonic frequencies, in general this will distort the input signal. Notwithstanding this distortion, constant absolute phase errors have no effect of ROCOF.

The attenuation factor will change with time and temperature due to component drifts, this will have no first order effect of ROCOF.

Electric and/or magnetic coupling between poly phase transducers will give-rise to "cross-talk" coupling of the signals channels.

2.2.3 Uncertainty Recommendations

Monte-Carlo simulations using the Roscoe algorithm [4] were carried and detail are given in Appendix 1. These simulations broadly confirm the above theory and the findings on transducers are summarised here.

Transducers has negligible impact on the uncertainty of ROCOF measurement. The errors in transducer ratio, phase does not impact ROCOF measurement. Even for a 1 Hz/s linear frequency ramp and considerable 0.1 radian phase error in the signal processing chain did not cause ROCOF errors greater than 10^{-6} Hz/s. Therefore there are no particular accuracy requirements for the specification of the transducer.

2.3 Analogue Front End

2.3.1 Description.

The analogue front end is signal conditioning electronics could, for example, contain an input buffer amplifier and over-voltage protection.

The input amplifier could be included to give the instrument a high input impedance so that it does not cause a loading of the transducer stage. This amplifier maybe given some gain to match the transducer output with the full range input of the ADC.

Overvoltage protection maybe included, for example incorporating clamping diodes such as Zener diodes or transient voltage suppression diodes. These should be specified to prevent damage to the ADC during an overvoltage fault.

2.3.2 Quality Considerations

The SNR contribution of the analogue front end should be aggregated with Eq. 1 and will degrade the FE and RE.

Distortion and non-linearity will add to the harmonic content which will be supressed by the digital filters.

Time delay and bandwidth are unlikely to be an issue at power frequencies.

Gain drift, for example caused by the temperature coefficients of the gain resistors in the amplifier will not affect FE and RE.

2.4 Anti-Aliasing Filter

2.4.1 Description

The anti-aliasing filter should attenuate all frequency components (e.g. harmonics and noise) above the Nyquist frequency, i.e above half the sampling rate (fs/2). Unfiltered or attenuated components above the Nyquist will be aliased to lower frequencies which could interfere with the wanted signal components.

2.4.2 Quality Considerations

Compared to a PMU or PQ analyser, the design specification for the anti-aliasing filter can be relaxed to allow the filter break point to be at a relatively low frequency. This is because a ROCOF measurement is only concerned with the power frequency fundamental and any attenuation of harmonics is to be welcomed. When ROCOF is part of a multi-parameter instrument, the requirements of other parameters will be dominant in the filter design. So for any dedicated ROCOF instrument with sampling frequency as recommended in Section 2.5.2, a passive single pole filter with a break point at say 250 Hz is a feasible low-cost solution. Relaxed filter designs have the added benefit of reducing the group delay (latency) caused by the filter.

2.5 Analogue to digital convertor (ADC)

2.5.1 Description.

The maximum working scale of the ADCs should not clip the signal and should have provision for at least 15 % overvoltage (10 % plus an allowance for harmonic crest factor), preferably at least 20-30 % overvoltage is a safer margin to allow for abnormal power system behaviour.

2.5.2 Quality Considerations

IEC 61869-9:2016 recommends a minimum of 14.4 kS/s sampling rate for the ADC. Increasing sample rate always decreases the effect of noise on the final measurement, since the linear noise amplitude density $\sqrt{L(f)}$ scales with $1/\sqrt{f_S}$, (see Eq. 6) as the noise is spread over a wider Nyquist band.

Experience shows that for these sampling rates, 12 to 13 effective number of bits (ENOB) is just about sufficient for ROCOF measurements, so a minimum of a 14 bit resolution ADC should be

sufficient. Given the wealth of available relatively inexpensive chips, a 16 bit device may the most appropriate choice to guarantee the required 13 ENOB.

ROCOF algorithms are relatively insensitive to ADC linearity errors. Any linearity errors will distort the sampled waveform and cause additional harmonics which will be readily rejected by the digital filters.

Some ADC designs (e.g. delta-sigma) apply ADC dithering techniques to improve linearity, which deliberately add white noise to the analogue signal. This should be considered in context of the SNR discussions in Section 2.1.

For a decent ADC, "aperture jitter" shouldn't be a problem, but the designer should check that it is not dominantly defining SNR (see section 2.1). The relationship of jitter to SNR is given in [1]:

$$SNR_{dB\ Jitter} = -20\log(2\pi f_C \cdot t_{RMS}) \qquad \text{Eq. 8}$$

Where, t_{RMS} is the ADC clock aperture jitter and f_c is the power system frequency. The result of Eq. 8 can be combined with the front end contribution to SNR (Eg.1), ultimately degrading the FE and RFE results in Eq. 6 and Eq. 7 respectively.

The four contributions 1) the front end white noise 2) ADC dithering noise 3) ADC quantisation and 4) jitter would be treated by summing (in an RSS manner) the SNRs as follows:

$$SNR_{dB} = -10\log_{10}\left(\sum_{i=1}^{4} 10^{\left(\frac{-SNR_{dB\_i}}{10}\right)}\right) \text{ dB} \qquad \text{Eq. 9}$$

For example:

$$SNR_{dB} = -10\log_{10}\left(10^{\left(\frac{-100}{10}\right)} + 10^{\left(\frac{-96.83}{10}\right)} + 10^{\left(\frac{-98.08}{10}\right)} + 10^{\left(\frac{-156}{10}\right)}\right) \qquad \text{Eq. 10}$$

SNR_{db} = -93.3dB

The result is then translated into effective number of bits using Eq. 1.

As a rule of thumb clock jitters at 30 ns or above could cause problems [5].

2.5.3 Uncertainty Recommendations

Monte-Carlo simulations using the Roscoe algorithm [4] were carried and detail are given in Appendix 1. These simulations broadly confirm the above theory and the findings on the ADC digitiser are summarised here.

The noise present in the signal and/or generated by the analogue front end and by the digitiser is the main contribution to the uncertainty of the ROCOF. Based on the simulations, by rule of thumb every 20 dB of noise leads to increase of uncertainty by one order of magnitude. For digitiser sampling signal with total SNR about 80 dB the uncertainty of ROCOF can be down to 0.1 %, for SNR about 100 dB the uncertainty can be down to 0.01 %.

The nonlinearity of analogue front end or ADC does not impact the uncertainty of the ROCOF.

The sampling frequency of the ADC has some impact on the uncertainty. If the sampling frequency is kept higher than 5 000 samples per second, the contribution to the uncertainty will be smaller than the contribution of noise of common digitiser.

2.6 Sampling Clock

2.6.1 Description.

A common clock can be used to supply all ADCs in a multi-phase instrument, so that the samples are taken at the same point in time.

2.6.2 Quality Considerations

As the clock defines the instruments unit of time, the clock accuracy is directly related to the frequency measurement accuracy. As the accuracy of even the cheapest quartz clocks is <50 ppm, it is not strictly necessary to have a GPS (or other source) conditioned clock, however accuracy can be readily assured in this way. The clock needs to be stable and have low "jitter". The clock frequency will be set by whatever sampling frequency is required. The sampling frequency will often be derived by dividing a higher frequency clock (e.g. 10 MHz) down to the required sampling frequency. As with the ADC jitter, the effect of sampling clock jitter translates to an increase in SNR according to Eq.8, which in turn cause the FE and RFE to degrade according to Eq. 6 and Eq. 7.

2.6.3 Uncertainty Recommendations

Monte-Carlo simulations using the Roscoe algorithm [4] were carried and detail are given in Appendix 1. These simulations broadly confirm the above theory and the findings on jitter are summarised here.

The noise contributed by the clock jitter for common digitisers is typically better than nanoseconds thus has negligible impact on the ROCOF uncertainty. A change in jitter from 1 ns to 10 ns will increase the SNR by 20 db, which will worsen RFE by an order of magnitude.

2.7 Summary of hardware effects on FE and RFE

The aggregated SNR contributions (e.g. Eq. 10) with give rise to FE and RFE errors as predicted by Eq. 6 and Eq. 7. SNR is related to ENOB by Eq. 1. Fig. 2 shows the relationships. RFE change is the dB_{10} change in RFE w.r.t the RFE for a SNR of -130 db.

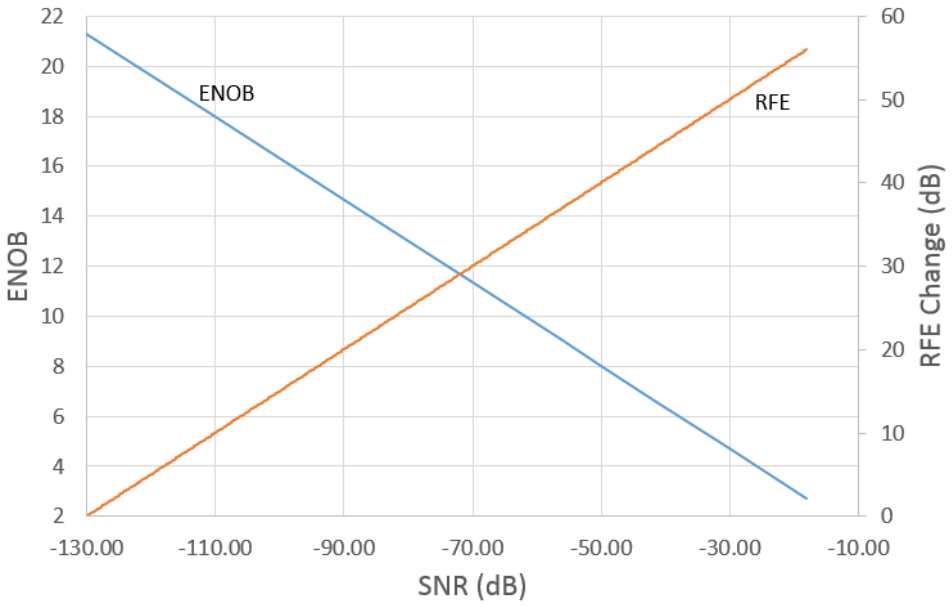

Fig. 2, Plot of ENOB and RFE Change against SNR

Summarising: a 10 dB change (order of magnitude) in RFE, results from a 20 dB change in SNR. Or every 6dB improvement in SNR, halves the RFE (as stated in Section 2.1).

3 Processing Part; Details of Each Component.

3.1 A real-time arithmetic processing engine

3.1.1 Description

Processing engines include digital signal processors, microprocessors, micro-controllers, and PCs (with real time data link).

3.1.2 Quality Considerations

The processor speed must obviously be considered and should be sufficient to carry out the required calculations for the given algorithm in real-time and dispatch the results in the chosen form. Real-time processing kernels maybe required as it is essential to maintain a constant stream of output results without variations in the update rate or variations latency of the results. The optimisation of the algorithm code for the actual hardware platform can be essential to maintain a constant stream of results.

The arithmetic processing engine will limit the size of processed number to a finite number of bits. Rounding the data to fit this finite word length will have an impact on the ROCOF results. Choice between single or double precision floating point arithmetic or fixed point calculations will need to be considered when selecting the processor and the requirements of the given algorithm and processing speed. Experience suggests 32-bit is “enough”, but clearly 64-bit is preferable if processor supports this for real time applications.

Memory size will also be determined by the chosen algorithm and the access speed must be sufficient for the update and latency requirements of the instrument. Using the tick-tock algorithm in [4], for a 26-cycle window, tuned to the lowest frequency (say 40 Hz), at 14.4 kSa/s, 4 buffers in parallel for 2 signals, for 3 phases, gives:

3*26/40*14400*4*2=224640 values

At 32-bit, 898560 bytes

At 64 bit 1797120 bytes

So some 2 MB would be required for this algorithm. The RAM needs to be fast access, since the buffer access is core to the signal processing algorithms. The organisation of the code and data storage is important to maximise execution speed; if memory locations are accessed in groups, rather than “dotted” throughout the memory space, this has a positive impact on execution speed. This makes best use of cache memory and minimises “cache misses”.

The processor will also be required to parse and dispatch the results to the communications or display stage.

3.2 Communications and display stage

3.2.1 Description

The ROCOF and frequency results could be used as part of the real time control of a power system and therefore must be dispatched in a reliable and time regimented fashion. They may also be logged and time stamped for diagnostic purposes.

3.2.2 Quality Considerations

Extensive commentary of communications and time stamping requirements is given the C37.118.1 PMU standard [1] and these guidelines may apply to a given ROCOF application and should be considered according to the intended application of the instrument.

Latency and response time are equally important in ROCOF applications as PMUs. In the case of some ROCOF applications, it is often necessary to provide reports much more often than standard PMU reports. For example, in converter-based systems new ROCOF measurements

are required at the full converter switching frequency (e.g. 2 to 4 kHz). In these applications, so long as the response time and latency are small enough, and the filtering good enough, users are generally unconcerned as to what the exact timestamp is.

3.3 Quadrature oscillator and heterodyne

3.3.1 Description

The heterodyne operation involves the multiplication of the digitised signal with cosine and sine waveforms at the fundamental power system frequency which are digitally generated from the quadrature oscillator.

The multiplication operation takes place at the sampling frequency resulting in two outputs, a real part and an imaginary part. This is a real time continuous version of the Fourier Transform kernel. These outputs can be integrated (summed) over one power system cycle to give the Fourier coefficients.

The resulting real and imaginary parts considered as a time series is an approximate sinusoidal function at the quadrature oscillator frequency which is set to be approximately the present power system fundamental frequency. Mixing products caused by the difference of the quadrature oscillator frequency from the power system frequency (which, in general, is constantly changing) will be present in the spectrum. Harmonics and interharmonics in the incoming signal will also be present and any amplitude modulation products caused by the voltage fluctuations.

This output is digitally filtered by the next stage to remove these unwanted frequencies.

3.3.2 Quality Considerations

Ideally, the frequency of the quadrature oscillator should match the frequency of the power system which is continuously changing. So a tuned oscillator can be used to track the power system frequency. This tuning can be driven by a feedback of the instruments frequency measurement, although care will need to be taken to avoid instability in this feedback loop. Parallel path heterodyne stages can be used to afford tracking and safeguard against instability, in such “tick-tock” systems [4], whist one path provides the heterodyning output, the other path’s filters settle on the present quadrature oscillator frequency, set to the last measured frequency. Once this dormant path has settled, the paths are switched and the newly dormant path is re-tuned to the latest frequency and is given time to settle.

The closeness of the quadrature oscillator frequency to the actual power system frequency will determine how many unwanted mixing products remain at the output from this stage. These products will cause the ROCOF result to vary and due to the nearness of the unwanted frequencies to the power system frequency, these cannot be well filtered. So good frequency matching the quadrature oscillator frequency to the actual power system frequency is highly desirable.

3.4 Digital Filters

3.4.1 Description.

Finite impulse response filters are used select the fundamental component and reject other frequencies such as harmonics, interharmonics and modulation products.

This stage may also perform the required integration over a fundamental cycle required to complete the heterodyne operation.

3.4.2 Quality Considerations

A paper describing the design of digital filter “Filter Designs for Frequency and ROCOF (Rate of Change of Frequency) Measurement Devices” has been submitted to IEEE TIM in March 2019. The paper identifies and defines the filter passband and stopband requirements in the context of the identified use cases and PQ scenarios. It then describes a filter architecture which can be added to the PMU heterodyne structure. This is based on cascaded boxcar (moving average) filters and a description is given as to how these can be applied in the context of the design rules.

This gives rise to several filter cascade configurations which attempt to meet the design rules, whilst satisfying the latency constraints of each use case.

3.5 Positive sequence calculator

3.5.1 Description.

In general it is required to measure ROCOF in three phase power. In such systems there may be a temptation to implement ROCOF measurement on a single phase only to save processing. However, there are advantages to implementing all three phases as this affords significant cancellation of the effect of balanced harmonics, improving the accuracy of the ROCOF measurement. The positive sequence component of the three phases can be readily calculated by the standard formula [6]. This can then be used to calculate frequency and ROCOF.

However, as discussed above, three-phase analysis allows a further SNR benefit of $1/\sqrt{3}$ (4.77 dB) to be gained by simply averaging the three results.

3.5.2 Quality Considerations

The symmetrical component transformation [6] can be used to calculate the positive sequence component.

Alternatively, the three values of frequency obtained on each phase can be averaged using a magnitude weighed average of the three calculated frequencies (for the calculation of frequency see Section 3.6). This average weighting is based on the phasor magnitude and has the advantage of eliminating the effect of unbalance as well as optimising the SNR as discussed above. ROCOF is then calculated from the weighted average frequency.

$$F_{av} = \frac{F_{L1} \cdot V_{L1} + F_{L2} \cdot V_{L2} + F_{L3} \cdot V_{L3}}{V_{L1} + V_{L2} + V_{L3}} \qquad \text{Eq. 11}$$

3.6 Phase and frequency differentiation.

3.6.1 Description.

Frequency is calculated by differentiating the measured phase. ROCOF is measured by differentiating the frequency.

The PMU standard C37.118.1 [1] recommends that the differentiation of phase be carried out using a weighted average of the past four phase differences (see equation C3 in C37.118.1). This is intended to smooth some of the variations in this generally noisy operation. Other methods use least squares methods or filtered outputs to reduce the variation.

It is important to ensure that the phase value used is not effected by principle value wrapping at two pi radians (360 degrees). Care needs to be taken to ensure transitions across this boundary are correctly handled in the calculation. For example, some algorithms may record two phases of 179 degrees followed by 181 degrees, do the phase difference is clearly 2 degrees. However, if 181 degrees wraps to -179 degrees to maintain the angle within the principle range, then the phase difference will erroneously be recorded as 358 degrees.

3.7 Data rate reduction - output decimator.

3.7.1 Description.

ROCOF algorithms can provide sample-by-sample updates of the F and R. Different applications require different update rates and the outputs are decimated to reduce the output rate of the instrument to the desired value.

Typical update rates are given in the PMU C37.118.1 standard and these may vary from once per half cycle (of the power system frequency) to once per 5 cycles as shown in Section C.7 of C37.118.1. As with any decimation process, a low-pass filter must be used to prevent aliasing [7]. Similar filters as used in Section 3.4 can be used to perform decimation.

Appendix- ROCOF Uncertainty Sensitivities using Monte Carlo Simulation.

4 Uncertainties Introduction

This appendix describes results obtained by simulating a Phasor Measurement Unit (PMU) using *pmusim* software developed by CMI. The Roscoe algorithm [4], was used to obtain ROCOF values.

A large number of input quantities are considered in *pmusim*. Every simulation variates one or two of these quantities. If not stated explicitly values of all other quantities were set to so-called *standard settings*. Numerical values of quantities of standard settings is listed in chapter 11. A detailed description of the model is in chapter 12.

Simple description of the modelled system follows. A three phase signal is generated and modulated according theoretical values. Next the *exact* signal is scaled according the parameters of a real transducer used in the Italian national metrology laboratory INRIM. Next, a filter is used to simulate the connecting cable between the transducer and the digitiser. Then the effect of the National Instruments PXI 4461 digitiser is simulated: a filter is used to simulate the bandwidth of the selected digitiser, the digitiser noise, distortion, jitter and quantisation is also simulated. The *Roscoe* algorithm is applied and result is compared to the theoretical values. This process is repeated and randomised according Monte Carlo method and the uncertainty of the results is estimated.

```
Signal generator → Transducer → Digitiser → ROCOF estimation
```

Thus the model is used to propagate uncertainties. The errors of the algorithm are obtained by comparing the output values to the theoretical values. If the uncertainty of the output value is smaller than the error, the accuracy of the algorithm is the most important factor.

The source code of the simulator is available at msira@cmi.cz.

4.1 Standard values of most important input quantities

To calculate dependencies of the output quantity, values of one or two input quantities were changed in simulations. Other input quantities were set to following values.

- Nominal sampling frequency: 14.4 kHz.
- Number of samples before *t0*: 3600.
- Nominal power frequency: 50 Hz.
- Peak magnitude: 3000 V.
- Noise in signal as one sigma of normal pdf: 1×10^{-7} V.
- Scale factor of transducer: 346.4101615138 V V^{-1}.
- Uncertainty of scale factor at 60Hz: 0.17 µV V^{-1}.
- Transducer output resistance: (200 ± 2) Ω.
- Transducer output capacitance: (1.0 ± 0.1) pF.
- Digitiser input resistance: (1.0 ± 0.1) MΩ.
- Digitiser input capacitance: (60.00 ± 0.60) pF.
- Noise of digitiser (without quantization noise) as one sigma of normal pdf: 2.8 µV.

- Uncertainty of gain of the digitiser at 50Hz: 3460 µV V^{-1}.
- Resolution of the digitiser: 24 bit.
- Range of the digitiser: 10 V.
- Digitiser low pass filter cut off frequency: 30 kHz.
- THD: (4.4 ± 0.5) × 10^{-6} dB.
- The limits of input frequency in the Roscoe algorithm: [40, 60] Hz.

5 Settling Time of the Roscoe ROCOF algorithm

The *Roscoe* algorithm needs some time to stabilise, and the time is dependent on the sampling frequency. Fig. 3 shows plots of total vector error (TVE) and ROCOF for static 50 Hz signal sampled at 14400 kHz. The designation *p. 003, Quantity,* refers to the value of the measurand (TVE). *LHQ* and *RHQ* refers to the Left/Right Hand Quantity (value of the measurand minus/plus the uncertainty).

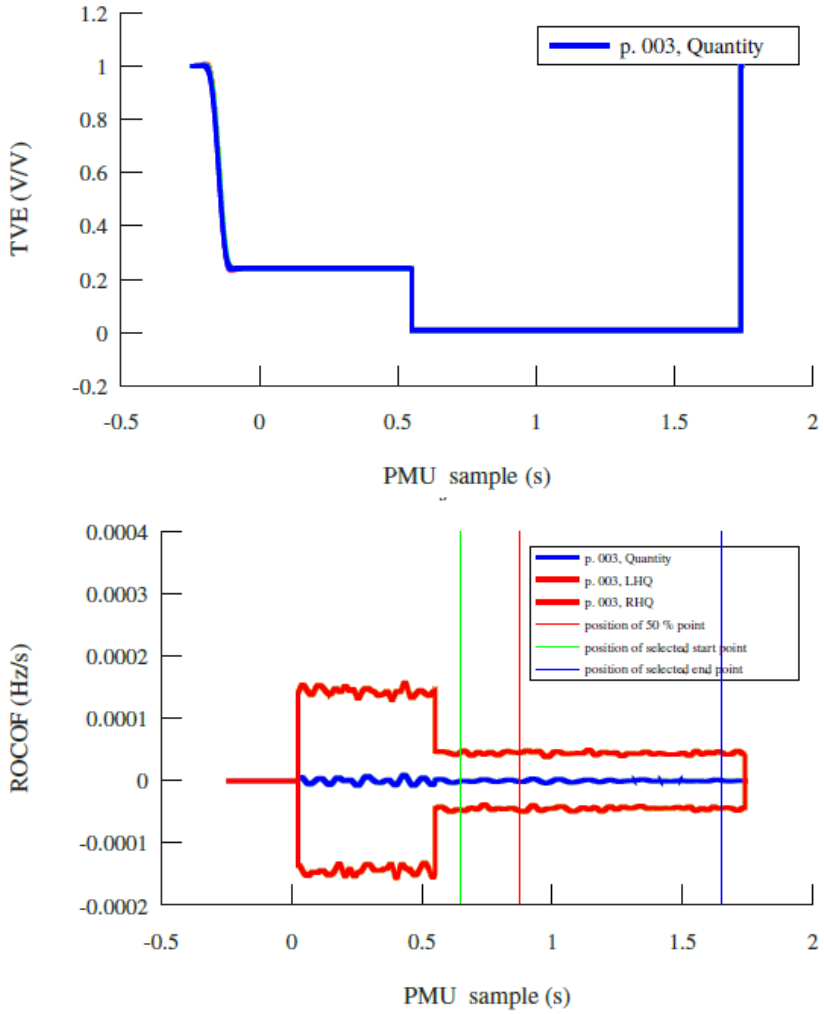

Fig. 3, Roscoe algorithm tuning phase, upper plot TVE, lower plot ROCOF.

During the first 0.25 s the *Roscoe* algorithm tunes itself to the power frequency. As can be seen in Fig. 3, the TVE and ROCOF uncertainty is increased until time t=0.6 s. After this time the result

is stable. The settling period lasts until the numerical value of time variable reaches a value of 0.6. The settling time does not depend on the length of the signal before t=0.6.

The discontinuity at the end of the simulation is due to the data stream ending. Therefore all results in following simulations have been calculated from period:

$$t \subset \langle 0.65, 1.65 \rangle \text{ s.}$$

Note: the behaviour of uncertainty below t=0.6 s is almost impossible to spot from a single calculation (Monte Carlo iteration). See Fig. 4 showing a single Monte Carlo iteration. Axes has the same range as in Fig. 3.

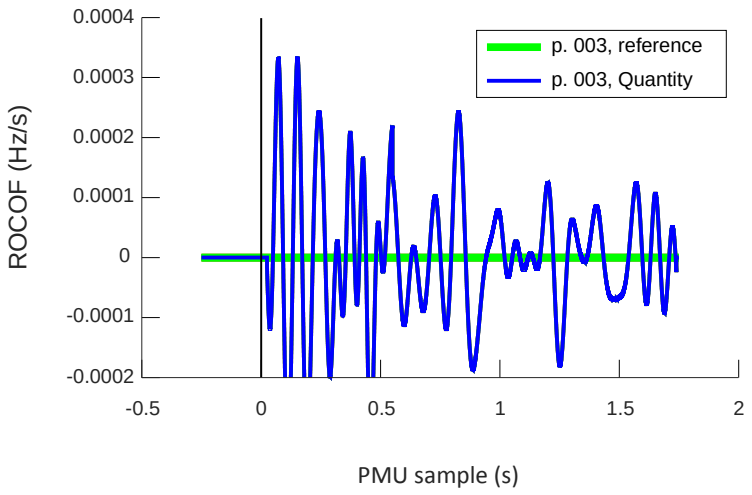

Fig. 4, A Single Monte Carlo iteration of the ROCOF calculation.

6 Uncertainty simulation probability density function (PDF)

Typically, the PDF has the characteristic of a normal distribution (20×10^3 Monte Carlo repetitions) as shown in Fig. 5.

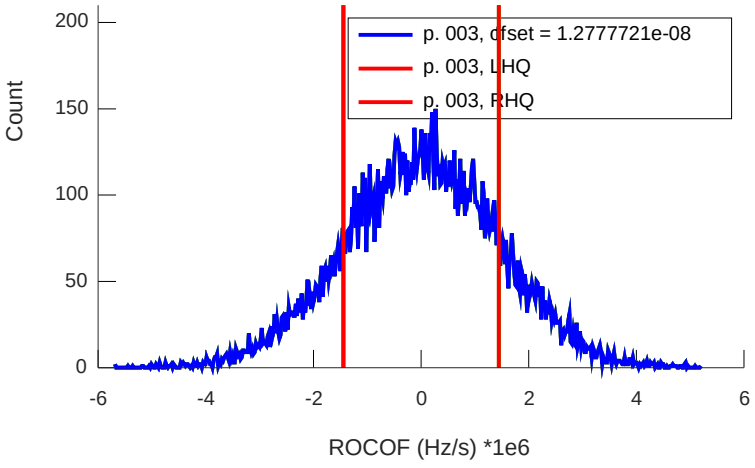

Fig. 5, PDF for 24 bit resolution ADC

However, if the bit resolution of the digitiser decreases too much, and the stochastic noise in the signal/digitiser remains at the same value, the pdf is no longer normal a as is the case for a 14 bit resolution ADC as shown in Fig. 6.

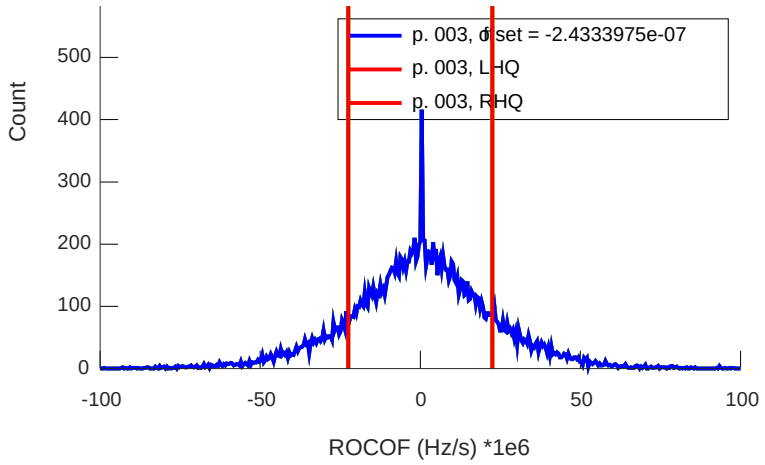

Fig. 6, PDF for 14 bit resolution ADC

As shown in Fig. 7, the PDF for a 12 bit resolution ADC is even more distorted.

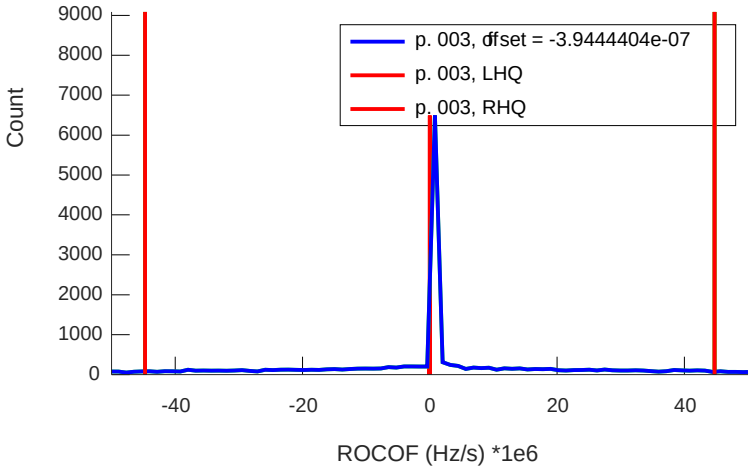

Fig. 7 PDF for a 12 bit resolution ADC.

So it can be seen that for low resolution ADCs, the introducion of substantial quantisation noise to the simulation, distorts the PDF.

However, the real digitizer has its stochastic noise that is usually higher than quantisation noise. This is described by so called Effective Number of Bits (ENOB), that takes into account both stochastic noise and bit resolution. Therefore the scenario as in Fig. 7, when digitiser is negligible compared to bit resolution, is typical only for digitisers with extremely low resolutions.

7 Uncertainty sensitivity of static signals

The figures in this section shows ROCOF and ROCOF uncertainty for the case of static three phase signal of frequency 50 Hz and amplitude 3 kV, without any modulation.

7.1 Digitiser noise

The stochastic noise of the digitiser (plotted on the x-axis as standard deviation of noise of normal distribution) has a large impact on the uncertainty (y-axis) as can be seen in Fig. 8. *LHU* and *RHU* refers to the Left/Right Hand Uncertainty of the Quantity (ROCOF).

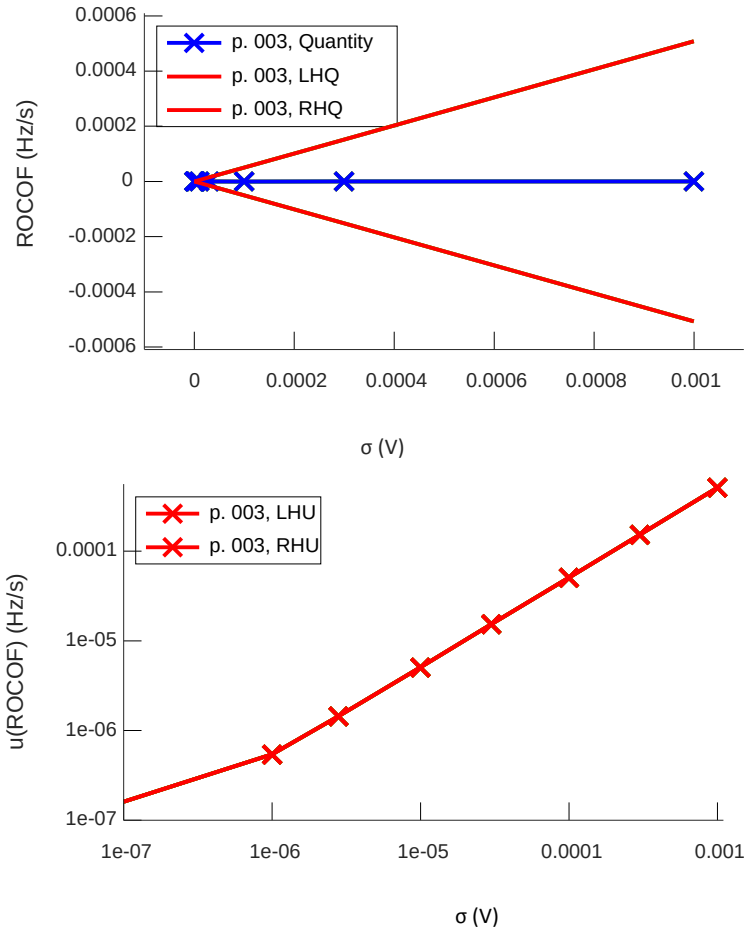

Fig. 8, The effect of increasing digitiser stochastic noise on the value of ROCOF (top plot) and the uncertainty of ROCOF (bottom plot) when using the Roscoe algorithm. Sigma σ(V) on the x-axis is the standard deviation of the noise. Axes of the bottom plot are log-log for better insight.

7.2 Signal noise

The noise in the signal has also large impact on the uncertainty. The signal noise is scaled down by the transducer, therefore for smaller values of noise the uncertainty caused by the digitiser noise prevails. The results are shown in Fig. 9.

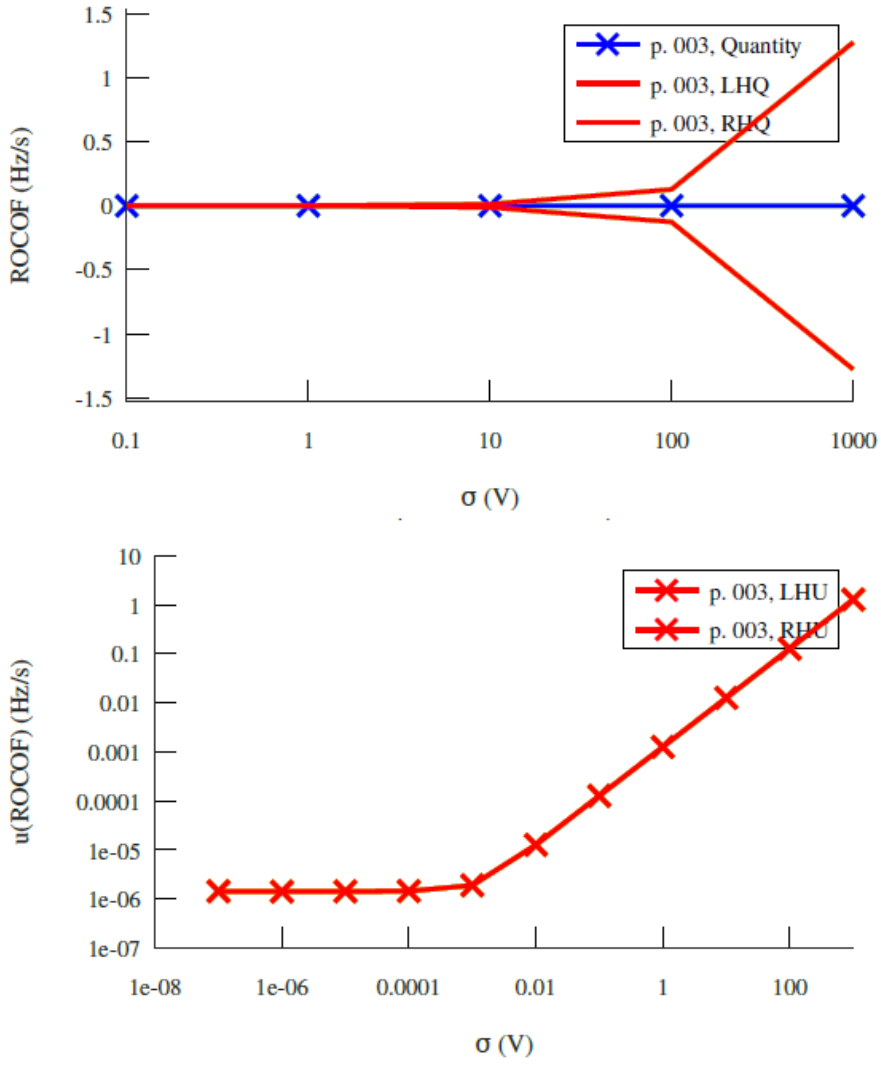

Fig. 9, Effect of signal noise on ROCOF and ROCOF uncertainty

7.2.1 Digitiser resolution

The resolution of the digitiser has substantial impact on the uncertainty. The uncertainty of ROCOF is logarithmically related to the bit resolution. For higher resolutions (greater than 22 bit) the stochastic noise of the digitiser is more important. This is shown in Fig. 10.

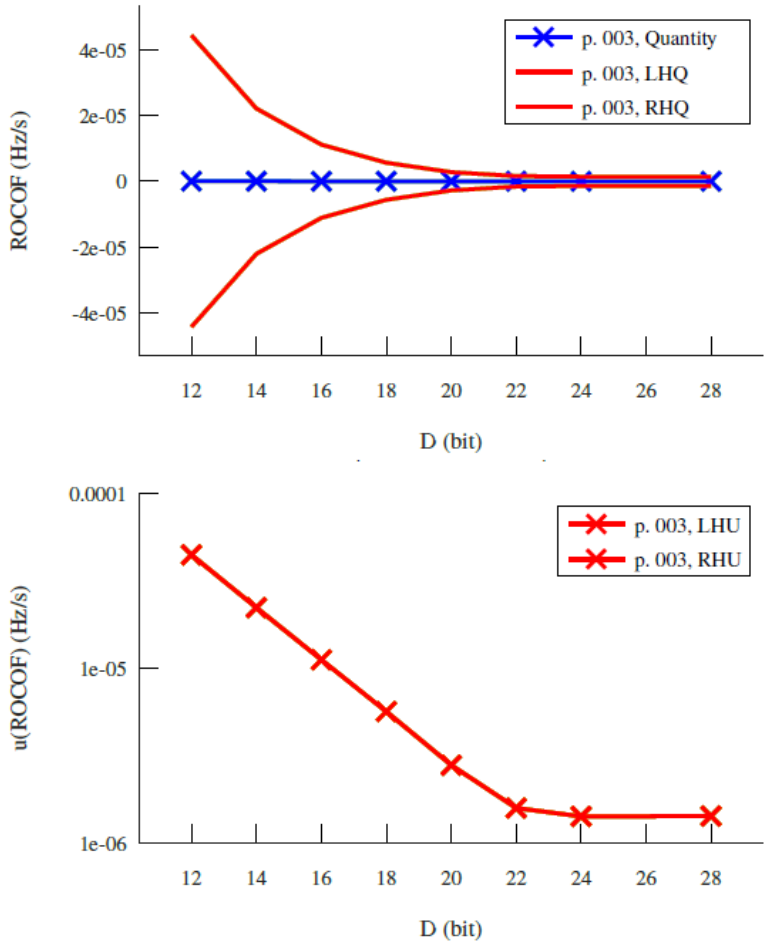

Fig. 10, Effect of digitiser resolution (x-axis) on ROCOF and ROCOF uncertainty.

Report Status: CO Confidential, only for members of the consortium (including EURAMET and the Eur Commission Services)

Delivery Report: D5

7.3 Digitiser resolution and digitiser noise

The resolution and stochastic noise are one of the most important factors. The Fig. 11 shows more complete view on the dependence of the ROCOF uncertainty on the digitiser resolution and digitiser (or source) stochastic noise. For increasing stochastic noise the contribution of the digitiser resolution is decreasing.

The resolution and stochastic noise are one of the most important factors. The resolution can be expressed as Signal to Noise Ratio (SNR) using:

$SNR_q = 1.761 + 6.021D$

where SNR_q is quantisation noise expressed in decibels and D is the digitiser resolution. The stochastic noise can be expressed as SNR_s using:

$SNR_s = 20 \log_{10}(A_{RMS}/\sigma)$

where SNR_s is stochastic noise of the digitiser, A_{RMS} is the amplitude of the signal at the digitiser input. The Fig. 11 shows the effect of digitiser resolution and digitizer stochastic noise (curves with different colour) on ROCOF uncertainty. Note the logarithmic y-axis. For increasing stochastic noise the contribution of the digitizer resolution is decreasing. The effect of the stochastic noise is more important than the effect of the quantisation noise.

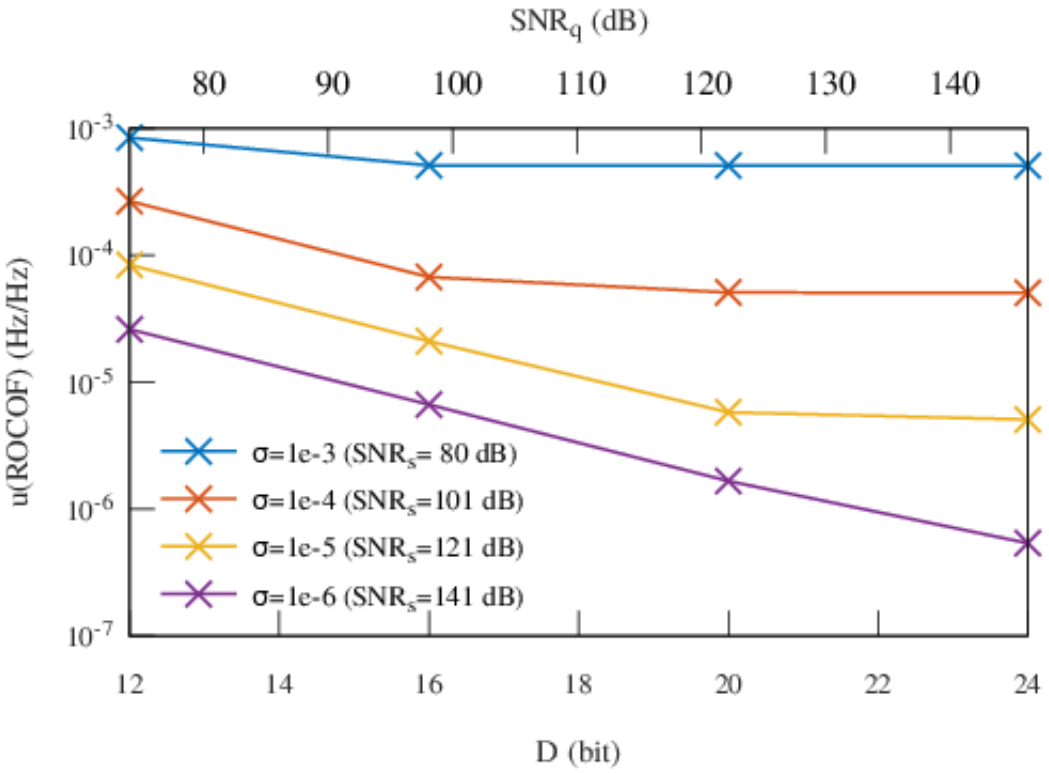

Fig. 11, Effect of digitiser resolution (D) and digitiser stochastic noise (curves with different colour) on ROCOF uncertainty. The value in the legend is the value of standard deviation of the digitiser stochastic noise. Note the logarithmic y-axis.

7.4 Signal frequency

The uncertainty of ROCOF (value of ROCOF was 0) slightly increases with the deviation of the signal frequency from the nominal value. The dependence on frequency is shown in Fig. 12, for a small range of frequencies. The limits of input frequency in the Roscoe algorithm was set to [40, 60] as shown in Fig. 13.

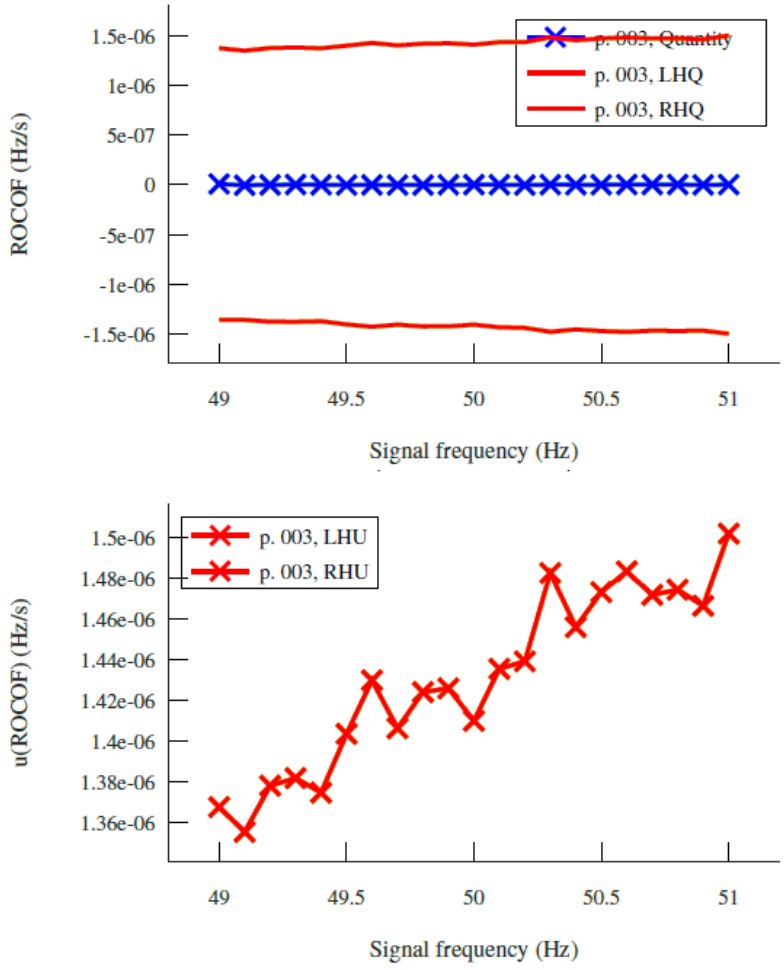

Fig. 12, Errors and Uncertainties caused be deviations of the power system frequency (49 Hz to 51 Hz) from nominal when using the tuned Roscoe algorithm.

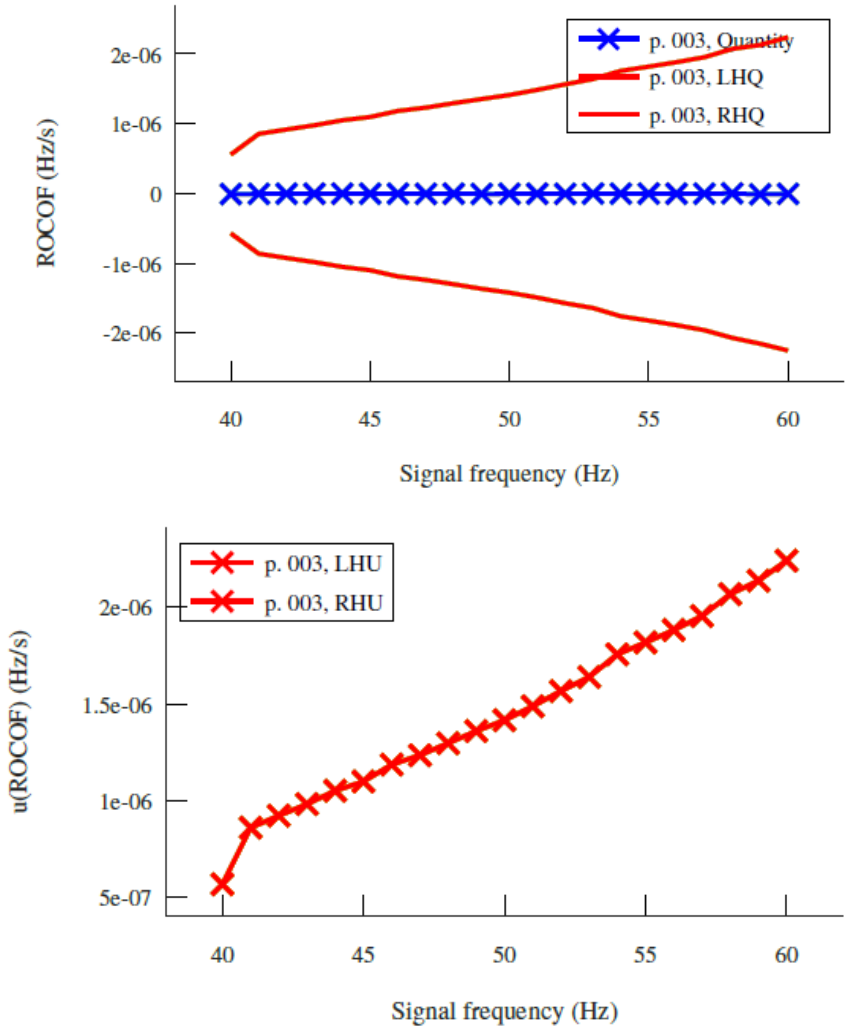

Fig. 13, Errors and Uncertainties caused be deviations of the power system frequency (40 Hz to 60 Hz) from nominal when using the tuned Roscoe algorithm.

7.5 Harmonics

The amplitude of third harmonic does not influence the value nor the uncertainty of ROCOF. Fig. 14 show x-axis as index, where indexes *i* determine the amplitudes of first and third harmonics:

i = 1, A_{3rd} = 0.3 V

i = 2, A_{3rd} = 3 V

i = 3, A_{3rd} = 30 V

i = 4, A_{3rd} = 300 V

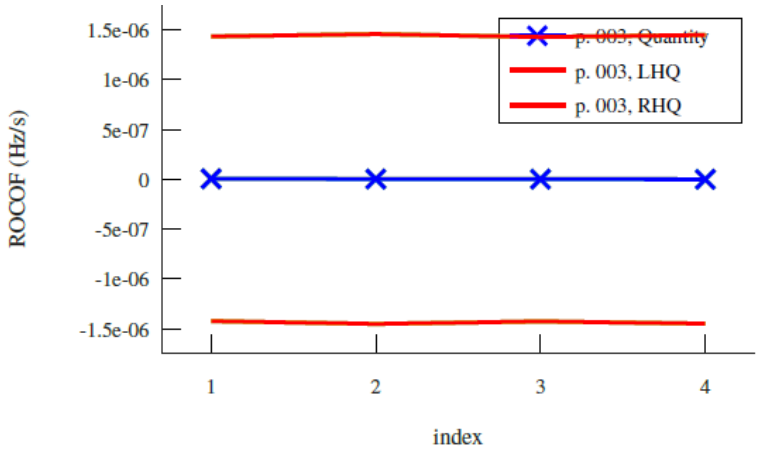

Fig. 14, Effect of various amplitudes of 3rd Harmonic

7.6 Interharmonics

If the interharmonic at frequency 75 Hz has very high amplitude (10 % of amplitude of main signal), as can be seen in Fig. 15, it can have an impact on the calculated value of ROCOF up to time 0.8 s (tested up to 10 s). There is no impact on the uncertainty at all.

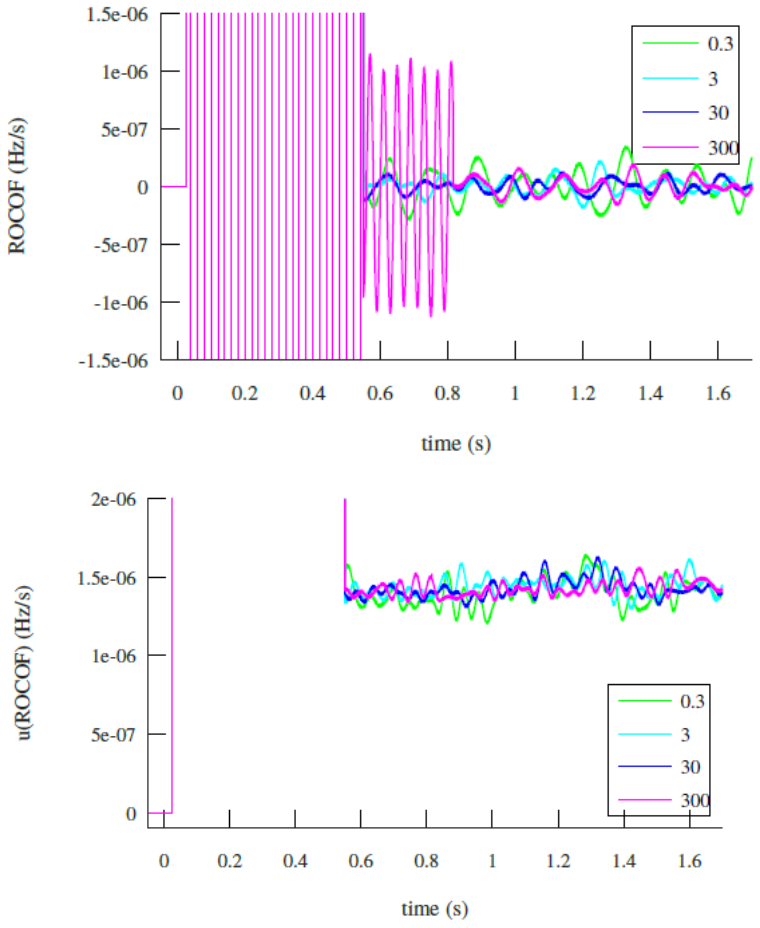

Fig. 15, Effect of an interharmonic at 75 Hz

The effect on the ROCOF value is because the 75 Hz interharmonic is not fully attenuated by the digital filter used in the Roscoe algorithm, the 75 Hz effectively appears in the *no-mans-land* between the pass-band where power system fluctuations need to be measured and the stop-band where harmonics and interharmonics need to be prevented from influencing the measurement. The problem can be solved by improving the filter masks for the algorithm.

7.7 Sampling frequency

As shown in Fig. 16, with decreasing sampling frequency the uncertainty of ROCOF increases non-linearly.

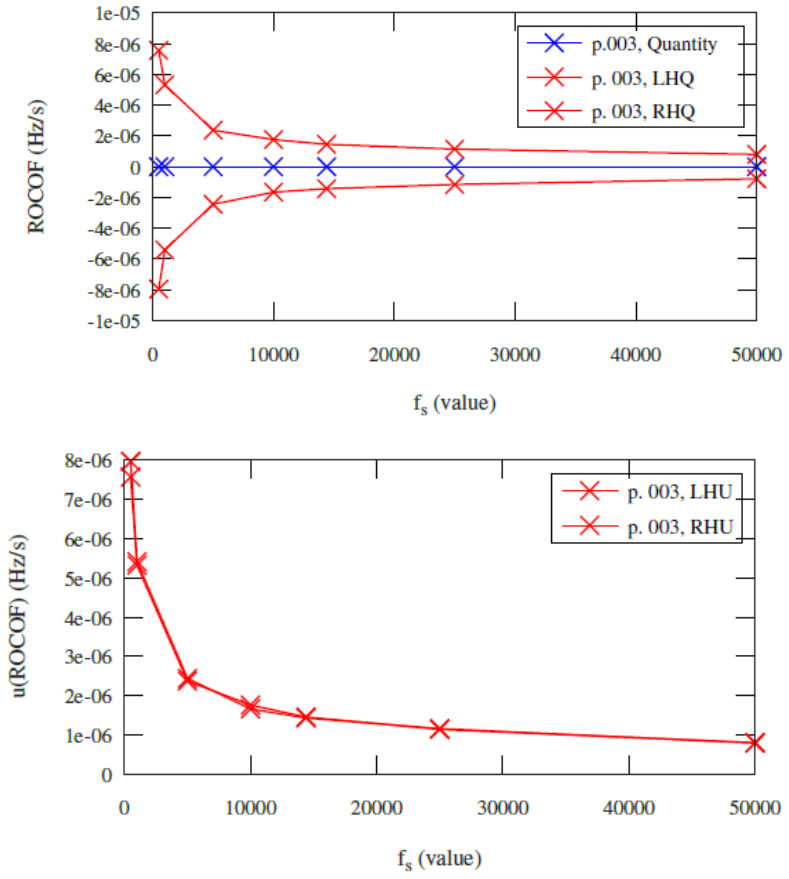

Fig. 16, Effect of sampling frequency

7.8 Unbalanced signals

The unbalanced signal does not have impact on ROCOF value, but has impact on the uncertainty. Fig. 17 shows the results when the amplitude of the first phase L1 was varied (phases L2 and L3 were kept at 3 kV).

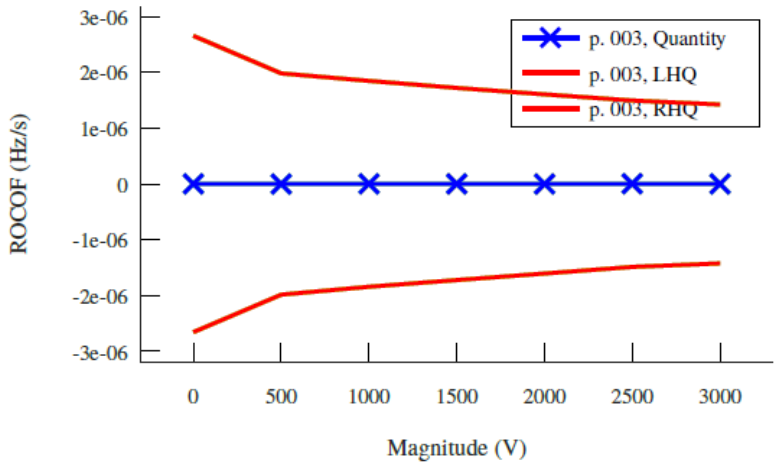

Fig. 17, Effect of unbalance by varying the amplitude of phase L1 as shown on the x-axis (L2 and L3 constant at 3 kV)

Fig. 18 shows the results when the amplitude of the first and second phase was varied (third one was kept at 3kV).

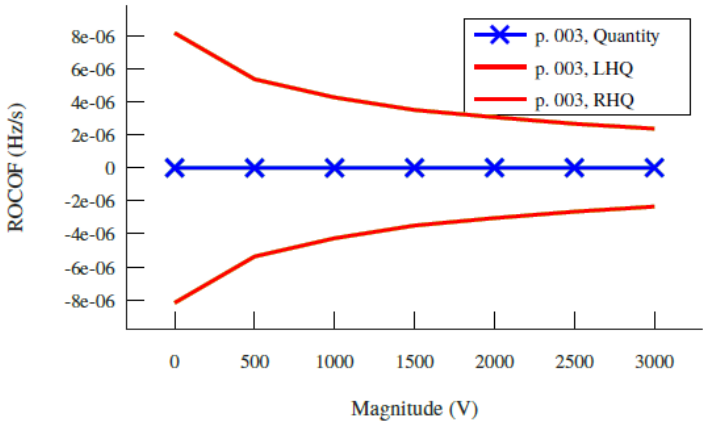

Fig. 18, Effect of unbalance by varying the amplitude of phase L1 and L2 together as shown on the x-axis (L3 constant at 3 kV)

These simulations were carried out using the positive sequence value of the three phase signal to calculate ROCOF. Advantage can be had of using the weighed mean of the three phase outputs to calculate ROCOF. The use of the weighed mean gives a considerable reduction of the effects of unbalance.

8 Uncertainty sensitivity of dynamic signals

8.1 ROCOF

In these simulations the signal is a linear chirp with various ROCOF values as shown on the x-axis of Fig. 19. In a small range of ROCOF, the ROCOF error is much smaller than uncertainty.

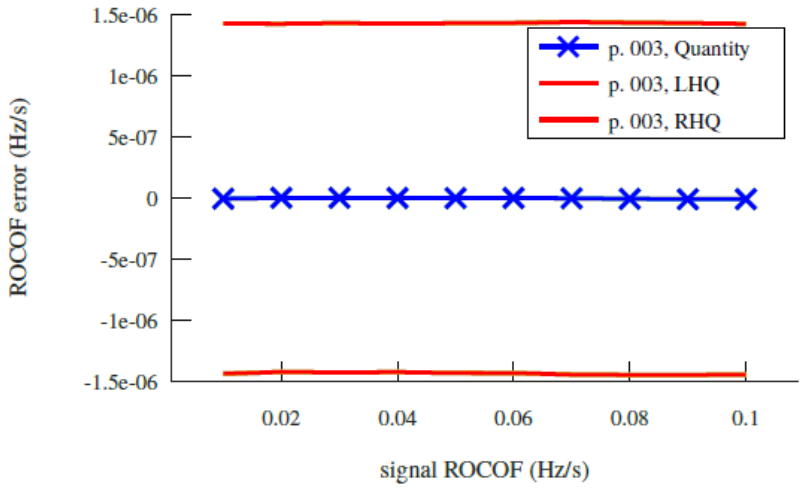

Fig. 19, Results for various linear chirp dynamic signals for smaller ROCOFs

For ROCOF greater than 0.4 Hz/s the error of ROCOF is larger than uncertainty as shown in Fig. 20.

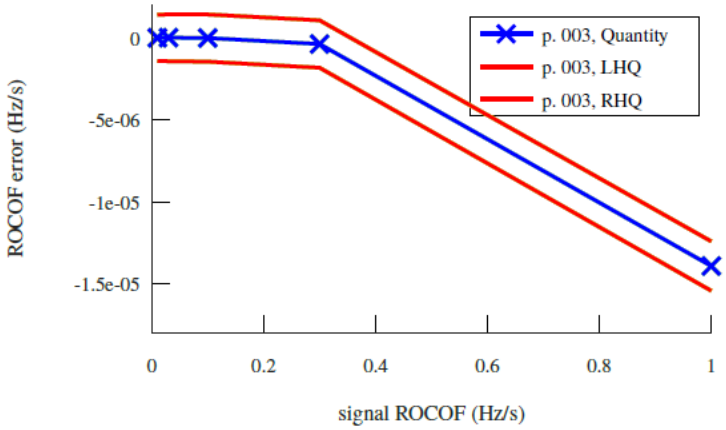

Fig. 20, Results for various linear chirp dynamic signals with ROCOF greater than 0.4 Hz/s

The error is linear in log-log scale in range of ROCOF 1 to 12Hz/s is shown in Fig. 21.

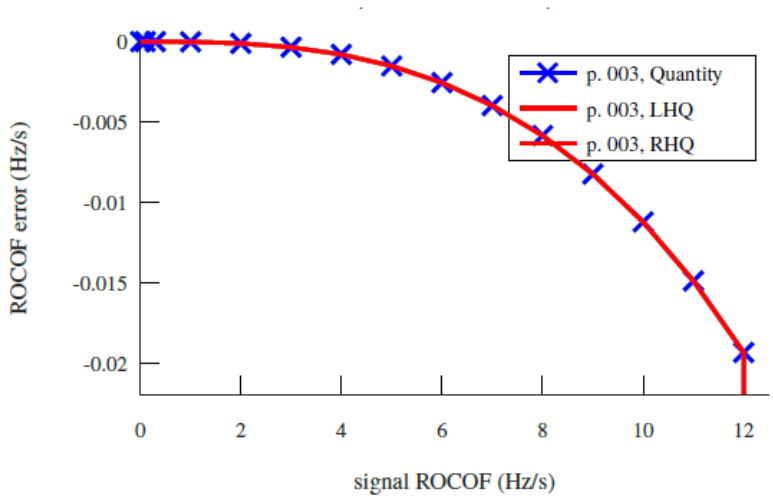

Fig. 21, Log-Log Scale for various linear chirp dynamic signals.

For ROCOF larger than 12 Hz/s the error is linearly increasing as shown in Fig. 22.

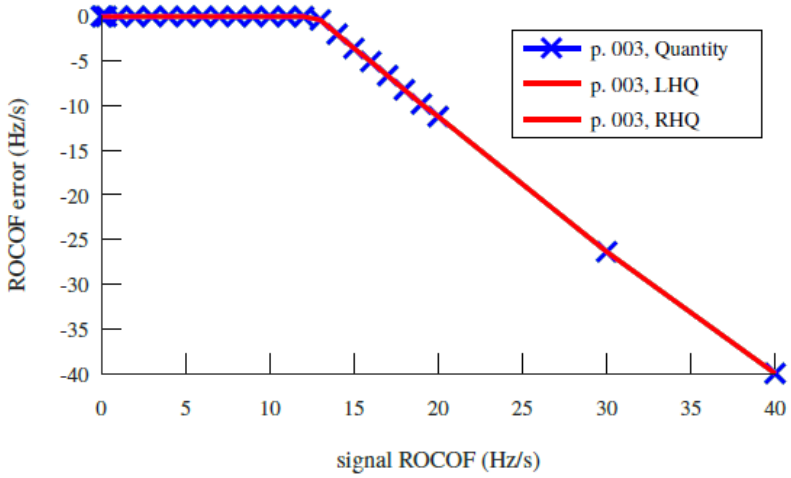

Fig. 22, ROCOF errors for various linear chirp dynamic signals with high ROCOF.

8.2 Magnitude step

The magnitude step creates peaks in value of ROCOF and uncertainty of ROCOF. Fig. 23 shows the time development for signal with magnitude step down of 3 V (in 3 kV) at time 1 s.

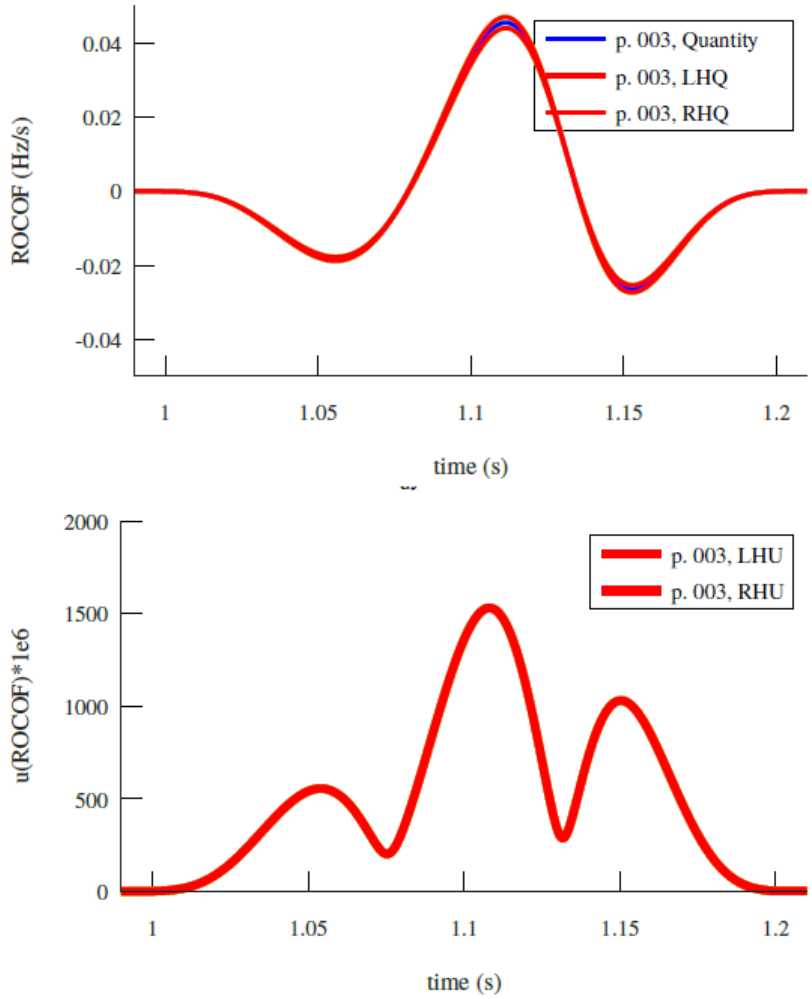

Fig. 23, Result for a magnitude step of 1 V.

Fig. 24 shows ROCOF for several values of the magnitude step ranged from 2 V to 600 V (relatively in 3 kV, 6×10^{-4} to 0.2 V/V) starting at time 1 s. During the step the ROCOF error is larger than uncertainty. The value of ROCOF stabilises in 0.2 s. The uncertainty is constantly increased after the step.

For each simulation, the development is shifted in the x-axis by 0.1 s for clarity. Because of the logarithmic y-axis, the absolute value of ROCOF is displayed

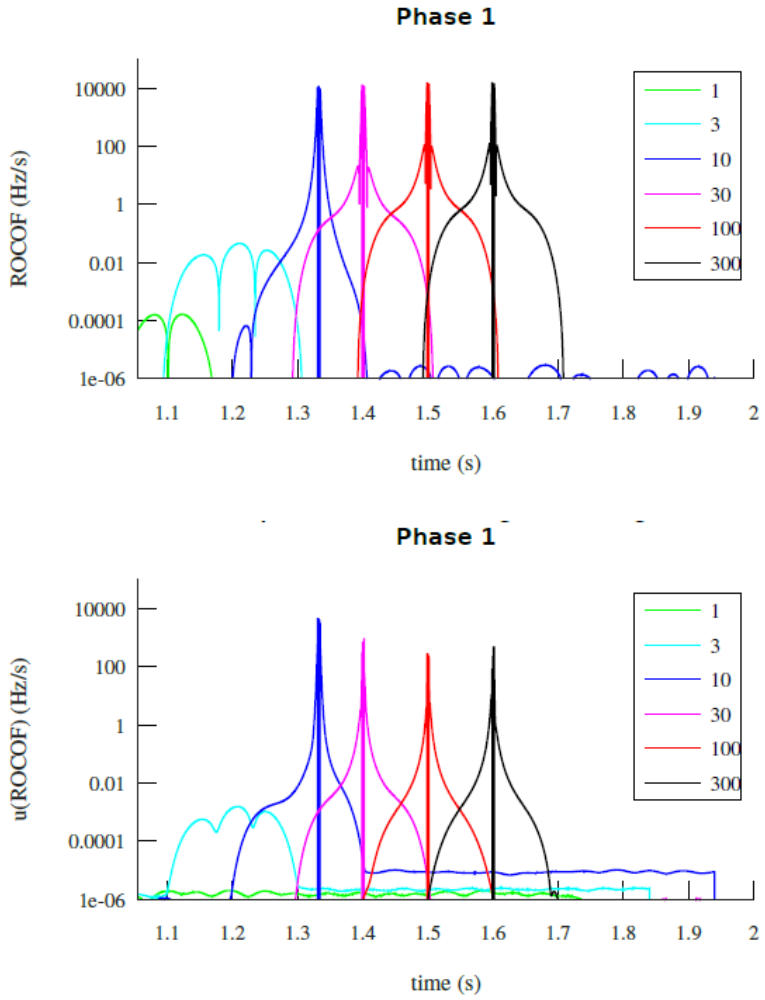

Fig. 24, Results for various size magnitude steps in volts. Time shifting on the x-axis is used for clarity.

8.3 Phase steps

The phase step (at time = 1 s) is applied to the test signal, ranging from 0.001 to 300 rad. As in the case of magnitude step, the error of ROCOF exceeds the uncertainty. Because of logarithmic y-axis, absolute value of ROCOF is displayed in Fig. 25.

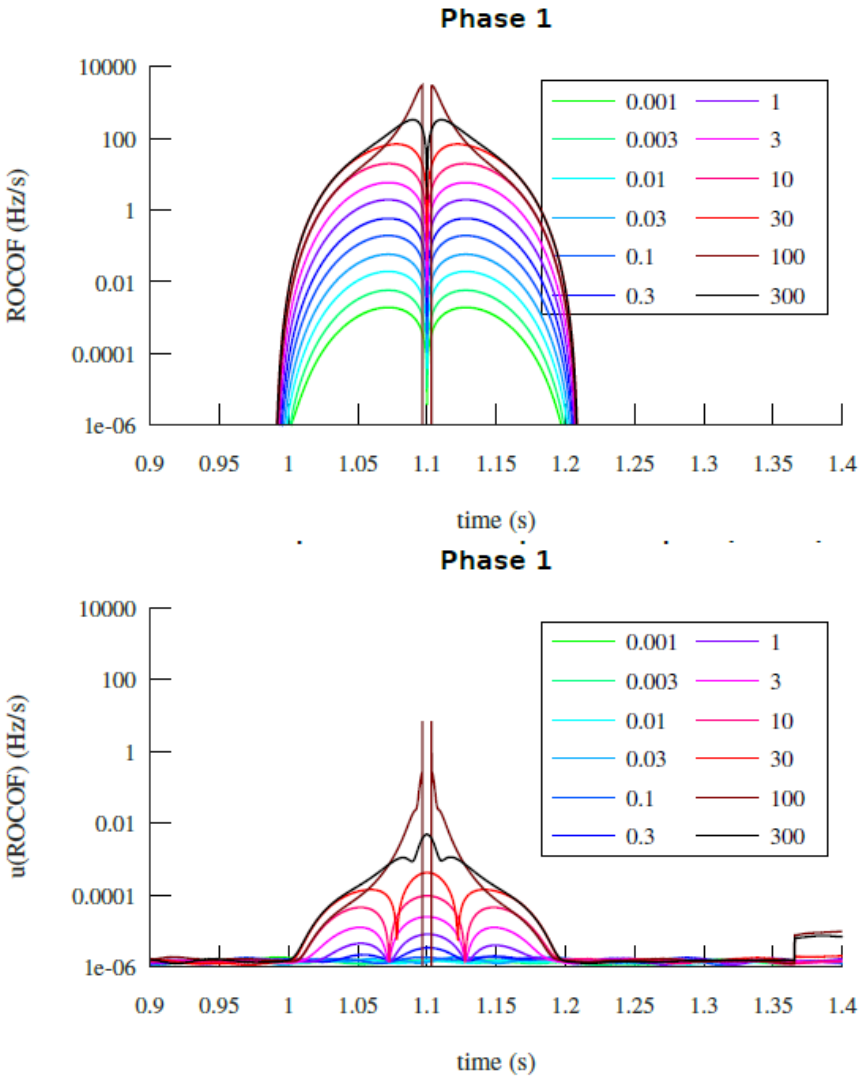

Fig. 25, Effect of various phase steps in radians.

8.4 Frequency step

The effect of a step change in frequency at time 1 s is shown in Fig. 26. As with phase steps (a closely related effect), the error of ROCOF exceeds the uncertainty of ROCOF. Frequency steps larger than 3 Hz cause increased uncertainty. The uncertainty settle down up to 0.7 s after the step occurrence.

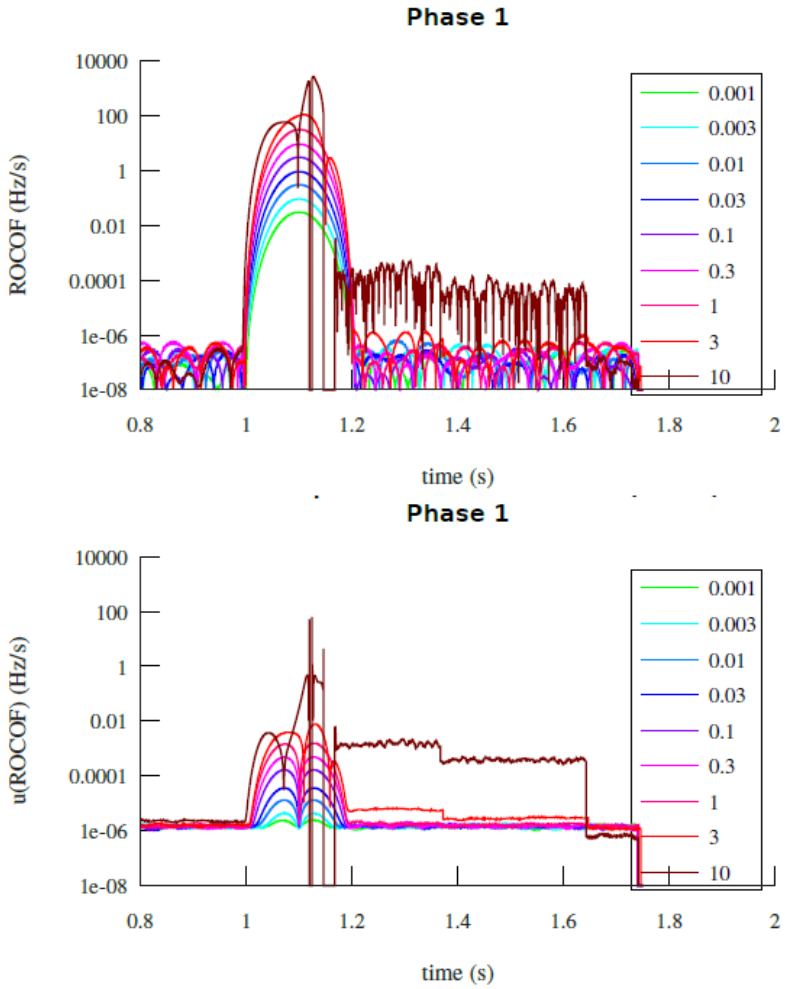

Fig. 26, Effects of various frequency steps

9 Uncertainty budget

The uncertainty budget for the standard settings.

Source of uncertainty	u(ROCOF), left		u(ROCOF), right	
	u(Hz/s)	% of RSS	u	% of RSS
Zeroed input uncertainties	0	0	3.7×10^{-14}	0
Bit. res.	0	0	4.5×10^{-14}	0
Digitiser stoch. noise	2.4×10^{-06}	100	2.4×10^{-06}	100
Signal noise	7.6×10^{-09}	0	7.6×10^{-09}	0
Transducer gain	6.5×10^{-09}	0	6.5×10^{-09}	0
Digitiser gain	6.5×10^{-09}	0	6.5×10^{-09}	0
RSS	2.4×10^{-06}		2.4×10^{-06}	
All sources	2.4×10^{-06}	0	2.4×10^{-06}	

10 Conclusion

- Algorithm requires some time to settle down.
- Stochastic noise (originating in signal, or digitiser) has substantial impact on the uncertainty.
- Resolution of the digitiser has substantial impact on the uncertainty for low noise cases.
- Signal frequency has small impact.
- Higher harmonics has negligible impact.
- Interharmonics has negligible impact.
- Sampling frequency has substantial impact for frequencies below 10 kHz.
- Unbalanced signals has small impact.
- For ROCOF larger than 0.4 Hz/s the algorithm error is higher than uncertainty (for selected setup).
- Steps in magnitude, phase or frequency cause algorithm errors of ROCOF higher than uncertainty (for selected setup).
- For selected setup, achievable uncertainty is about 3µHz/s for simple static signal. This value does not include hypothethical disturbances in the measured signal.

11 Values of standard settings used in the Monte Carlo simulations

A list, values and short description of quantities used in the simulations and their uncertainties follows. These values have been used for all calculations unless otherwise stated. Settings were prepared for several model cases. Two digitisers have been considered: the National Instruments PXI 4461 and the National Instruments PXI 5922. Sampling frequencies of both digitisers are different and this would impact on the ease of the comparison of uncertainty budgets and sensitivity analysis. Therefore the sampling frequency of PXI 5922 was set to the same value as of PXI 4461. The impact of sampling frequency is considered separately.

11.1 Acquisition parameters

- Nominal sampling frequency: 204.8×10^3 Hz
- Oversampling multiplier: 10
- Total number of samples acquired: 103.4×10^3
- Number of samples before t_0: 1×10^3
- PMU frames per second: 50
- Number of THD repeated measurements: 50

11.2 Source signal parameters

- Nominal power frequency: 50 Hz
- Signal harmonics:
  - rank: 1
  - RMS magnitude: 3000 V
  - Phase: 0 rad

- Original noise in signal as one sigma of normal pdf: $1e^{-7}$ V
- No frequency, phase or amplitude modulation.

11.3 Transducer parameters

- Nominal dividing ratio (scale factor): 346.4101615138 V/V
  - Frequency response - amplitude ratio error:
  - Frequency of measured points (Hz): *f*
  - Absolute ratio errors at measured points (V/V): *ε*
  - Absolute uncertainties of abs. ratio errors (V/V): *u(ε)*
  - Correlation of uncertainties: 0.5

f Hz	ε V/V	$u(\varepsilon)$ V/V
60	2.6476499617	0.1758629842
100	3.3136262131	0.1765346911
200	4.1623380956	0.1773925196
500	4.8219045359	0.178060631
1000	6.286440587	0.1795486722
2000	12.3320012293	0.1857566811
3000	23.7364737347	0.3955098074
4000	46.132598818	0.4448193904
4500	66.5885811092	0.4923878886
5000	104.029293161	0.5857096391
5500	229.4298114691	0.9572228868
6000	-85.123854813	0.1970802821
6500	-17.7755537135	0.3117713486
7000	32.5871213686	0.4146501668
8000	121.9864630492	0.6333407926
8500	189.1103448231	0.8278694127
9000	300.4701089428	1.2079750443
10000	806.7737827594	4.6066771383
12000	-165.6542805865	0.1226134352
14000	-238.8951390907	0.0467171315
16000	-190.3211167075	0.1054984254

- Frequency response - phase displacement:
  - Frequency of measured points (Hz): f
  - Errors at measured points (rad): Φ
  - Absolute uncertainties of errors (rad): u(Φ)
  - Correlation of uncertainties: 0.5

f Hz	Φ µrad	$u(\Phi)$ µrad
20	0.016248	100
40	0.011175	100

60	0.008915	100
100	0.005994	100
200	0.004156	100
500	0.000778	100
1000	-0.000472	100
2000	-0.002588	200
3000	-0.002813	200
4000	-0.002233	200
4500	0.006698	200
5000	0.020762	200
5500	0.138029	200
6000	0.627432	200
6500	0.108059	200
7000	0.067382	200
8000	0.083492	200
8500	0.119896	200
9000	0.198615	200

11.4 Cable parameters

- Transducer output resistance: (200 ± 2) Ω
- Transducer output capacitance: (1 ± 0.01) × 10^{-12} F
- Cable resistance: (0.4 ± 0.004) Ω
- Cable inductance: (2 ± 0.02) × 10^{-6} H
- Cable capacitance: (0.2 ± 0.002) × 10^{-9} F
- Digitiser input resistance: (1 ± 0.01) × 10^{6} Ω
- Digitiser input capacitance: (60 ± 0.60) × 10^{-12} F

11.5 Digitiser parameters

- Uncorrelated part of jitter: (0 ± 2) × 10^{-12} s
- Correlated part of jitter (s): (0 ± 10^{-6}) s
- Noise of digitiser as one sigma of normal pdf: 2.8 × 10^{-6} V
- Gain of the digitiser at 50 Hz:
    - relative errors at measured points: 0 V/V
- Absolute uncertainty of relative errors: 3460 × 10^{-6} V/V
- Drift of the gain of the digitiser at 50 Hz:
    - Change of relative error per second: 0.415 × 10^{-6} V/(Vs)
    - Absolute uncertainty of change of relative error per second: 0.208×10−6 V/(Vs)
- Phase error of the digitiser at 50 Hz:
    - Error at measured points: 0 rad

    - Absolute uncertainty of error: 174 × 10^{-6} rad
- Resolution of the digitiser: 24 bits
- Range of the digitiser (symmetric): 10 V
- THD: (4.4 ± 0.5) × 10^{-6} dB

12 Monte Carlo Analytical model

This section describes analytical models used in the Monte Carlo simulation program *pmusim*.

12.1 Transducer – Current transformer

12.1.1 Source of calibration data

Transducer properties are based on a calibration of a commercial inductive voltage transducer delivered by INRIM [8] in an Excel sheet.

Description of cells in sheet:

- SF(V/V): scale factor.

$$\frac{U_{\text{in}}}{U_{\text{out}}} = \frac{U_{\text{primary}}}{U_{\text{secondary}}} = SF_{\text{nominal}} = \frac{\frac{20\ \text{kV}}{\sqrt{3}}}{\frac{100\ \text{V}}{3}} = 346.4101615$$

- ε(μV/V): ratio error – named as error in excel sheet, but International vocabulary of metrology explicitly states error is "measured quantity value minus a reference quantity value".

$$\varepsilon(\mu\text{V/V}) = \frac{SF_{\text{nominal}} - SF}{SF} 10^6$$

- $u(\varepsilon)$(μV/V): ratio error uncertainty.

$$\varepsilon = \frac{SF_{\text{nominal}} - SF}{SF} \rightarrow SF = \frac{SF_{\text{nominal}}}{\varepsilon + 1} \rightarrow u(SF) = -\frac{SF_{\text{nominal}}}{(\varepsilon + 1)^2} u(\varepsilon)$$

- Φ(μrad): phase displacement.
- u(Φ)(μrad): phase error uncertainty.
  The scale factor and ratio error of measured transducer is shown in Fig. 27.

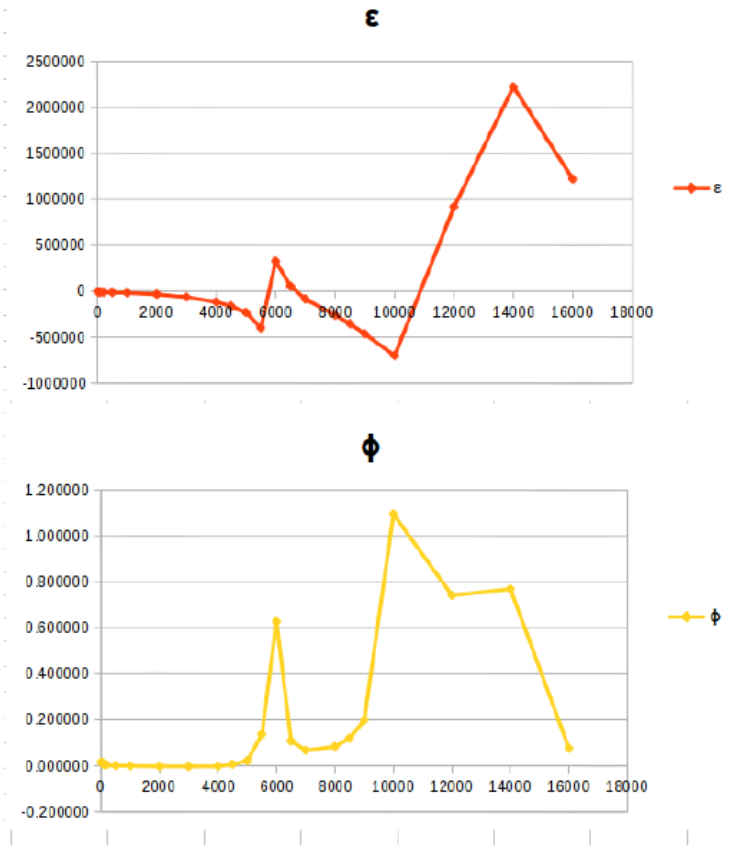

Fig. 27, scale factor and ratio error of measured transducer

12.1.2 Input values

Values set in the MATLAB model: *standard_settings.m*:

- *trans.R.v*: R, nominal dividing ratio (scale factor) (V/V).

  $$R = SF_{\text{nominal}}$$

- *trans.G.v*: G, absolute ratio error (V/V).

  $$G = SF - SF_{\text{nominal}}$$

- *trans.P.v*: P, absolute phase error (rad).

  $$P = \Phi - 0$$

12.1.3 Simulation

Transducer is simulated in such a way first a reference data is generated by Software Platform developed in the SmartGrids I EMPIR project. It means a theoretical values and a waveform is generated as appears at the input of the transducer. Only theoretical values of output quantities (ROCOF) are used and the samples of the waveform itself are not used in following calculations. Next a new waveform is generated and scaled according parameters modified by properties of the transducer.

This second waveform is used subsequent calculations

Simulation of transducer – equations in MATLAB file *transducer.m*.

$$A_{\text{out}} = \frac{A_{\text{in}}}{R + G}$$

$$ph_{\text{out}} = ph_{\text{in}} + P$$

- A_{in} – amplitude of signal component at the input of the transducer
- A_{out} – amplitude of signal component at the output of the transducer
- ph_{in} – phase of signal component at the input of the transducer
- ph_{out} – phase of signal component at the output of the transducer

12.2 Matching

12.2.1 Source of calibration data

The values of transducer output impedance is based on information obtained from INRIM, see B.1.1. The values of connecting cable impedance is based on values measured in CMI of typical 50 Ω cable. The values of digitiser input impedance is based on measurements or datasheet of selected digitiser.

12.2.2 Input values

Values set in standard_settings.m.

- match.T_R: T_R – transducer output resistance (Ω).
- match.T_C: T_C – transducer output capacitance (F).
- match.C_R: C_R – cable resistance (Ω).
- match.C_L: C_L – cable inductance (H).
- match.C_C: C_C – cable capacitance (F).
- match.D_R: D_R – digitiser input resistance (Ω).
- match.D_C: D_C – digitiser input capacitance (F).

12.2.3 Simulation

The system is simulated as Linear Time Invariant system (*LTI)* according to the electrical model shown in Fig. 28.

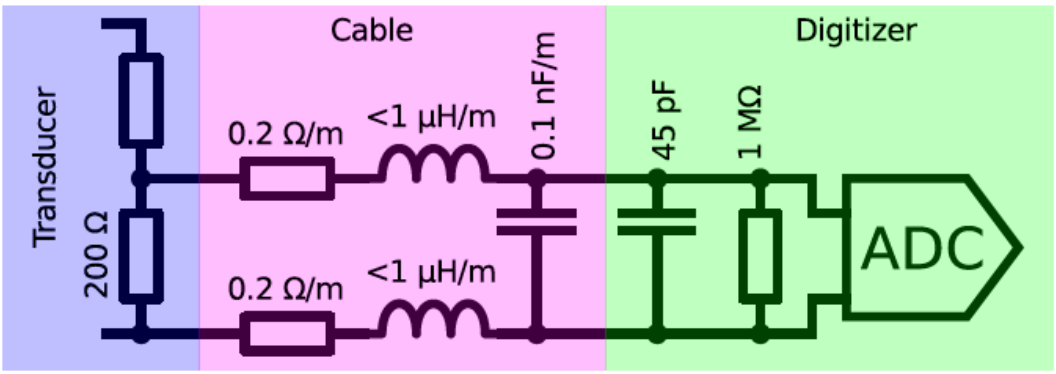

Fig. 28, System model of Linear Time Invariant system

$$LTI = \frac{D_R}{Z}$$

$$Z = s^2 (C_L C_C D_R + C_L D_C D_R + C_L C_C D_R + C_L D_C D_R) + s (C_R C_C D_R + C_R D_C D_R + C_R C_C D_R + C_R D_C D_R + C_L C_L) + D_R + 2C_R$$

Fig. 29, System model of Linear Time Invariant system

12.3 Digitiser – time base

12.3.1 Source of calibration data

The jitter of the digitiser is based on the datasheet of the NI PXI unit.

12.3.2 Input values

Values set in standard_settings.m.

- digit.J_u: J_u – uncorrelated part of jitter.
- digit.J_c: J_c – correlated part of jitter.

12.3.3 Simulation

Jitter and other specifics of the digitiser time base is simulated as interpolating the waveform. The input waveform is oversampled to increase the precision of the interpolation.

$$J = J_u + J_c$$

$$t = \langle n, N - n - 1 \rangle \cdot \frac{1}{f_s} + J + t_{ps}$$

Where *t* is time of samples, t_{ps} is phase shift caused by digitiser phase error (see above). The waveform is interpolated at time *t*.

12.4 Digitiser – gain

12.4.1 Source of calibration data

Value of the gain of digitiser is based on datasheet of particular digitiser.

12.4.2 Input values

Values set in standard_settings.m.

- digit.G.f: frequency of the measured calibration point of the digitiser (Hz).
- digit.G.v: G – relative error at measured point (V/V).
- digit.G_d: G_d – drift of the digitiser gain (V/(Vs)).
- S_{in} – signal at the input of the digitiser (V).
- S_{out} – sampled point of the digitiser (V).

12.4.3 Simulation

Only one gain value (at 50 Hz) is simulated.

$$E = G + \frac{G_d \cdot i}{f_s}, i = 1 \ldots M$$

$$S_{out} = S_{in}(1 + E)$$

M is the total number of samples.

12.5 Digitiser – phase error

12.5.1 Source of calibration data

The value is based on the phase channel mismatch of a digitiser and its value is taken from datasheet of particular digitiser.

12.5.2 Input values

Values set in standard_settings.m.

- digit.P.f: frequency of the measured calibration point of the digitiser (Hz).
- digit.P.v: P – absolute phase error at measured point (V/V).

12.5.3 Simulation

P is based on the inter-channel phase mismatch of the digitiser. Only one value at 50 Hz is simulated. Phase error cause time shift t_{ps} of the sample time. Phase shift is applied together with jitter (see below).

$$t_{\mathrm{ps}} = \frac{P}{2\pi} \cdot \frac{1}{50}$$

12.6 Digitiser – THD

12.6.1 Source of calibration data

Value of the THD of digitiser is based on datasheet of particular digitiser.

12.6.2 Input values

Values set in standard_settings.m.

- digit.THD.v: THD – Total Harmonic Distortion, (V/V).

12.6.3 Simulation

Transfer function simulating THD of the digitiser is modelled by quadratic function.

$$S_{\mathrm{out}} = c \cdot S_{\mathrm{in}}^2 + b \cdot S_{\mathrm{in}} + a$$

where:

- a, b, c – coefficients of the transfer function.
- Sin – signal at the input of the digitiser (V).
- Sout – sampled point of the digitiser (V).

For a symmetric digitiser range $\langle -R,R \rangle$ and this quadratic function *b* is always 1 Coefficients are searched iteratively by constructing testing sine waveform, applying coefficients and evaluating THD until the THD precision is below 1 % of THD uncertainty.

12.7 Digitiser – noise

12.7.1 Source of calibration data

Value of the RMS noise of digitiser is based on datasheet of particular digitiser.

12.7.2 Input values

Values set in standard_settings.m.

• digit.noise: D_N – noise of the digitiser as one sigma of Gaussian noise.

12.7.3 Simulation

A random number of normal distribution function is added to every sample.

12.8 Digitiser – quantisation

12.8.1 Source of calibration data

Value of the bit resolution of digitiser and range is based on datasheet of the particular digitiser.

12.8.2 Input values

Values set in standard_settings.m.

- digit.Dn.v: D_n – bit resolution of the digitiser (bits).
- digit.R.v: R – symmetric range of the digitiser (V).

12.8.3 Simulation

Simulated by simple quantisation of the waveform.

$$S_{\text{in}} > R = R$$

$$S_{\text{in}} < -R = -R$$

$$l = 2^{D_n} - 1$$

$$S_{\text{out}} = \text{round}\left(S_{\text{in}} \frac{l}{R}\right) \frac{R}{l}$$

12.9 Digitiser – filter delay

12.9.1 Source of calibration data

Value of the filter delay of digitiser and range is based on datasheet of particular digitiser. However digitiser includes the delay already into the reported time of the sample, therefore this delay is not included in calculations at all.

12.9.2 Input values

Values set in standard_settings.m.

- digit.filtdelay.f: ranges of sampling frequencies of particular filter delay
- digit.filtdelay.v: filter delay in number of samples.

12.9.3 Simulation

Waveform is delayed (shifted) appropriate number of samples. Waveform is padded from left by constant value equal to the first real sample.

12.10 THD calculation

The theoretical value is calculated from harmonic amplitudes of source waveform. Software platform used for generation of the waveform can generate modulated waveforms, however none of implemented modulations can affect THD (amplitude modulation affects all harmonics proportionally). Therefore theoretical value of THD has no time development and is constant for whole generated waveform.

A calculator of THD called *THD_Meter* developed in CMI [9] is used. This algorithm is based on calculation of spectrum, identification of peaks, and correction of outputs and uncertainty calculation based on the noise in the data. Usually more than one measurement is used to calculate THD by this algorithm. This algorithm do not require coherent measurement.

Several waveforms generated by Monte Carlo procedure are saved into temporary files and main script of THD_Meter thd2.m is started.

THD of this definition is calculated:

$$\mathrm{THD}_{k_1} = \frac{\sqrt{A_2^2 + A_3^2 + A_4^2 + \cdots}}{A_1}$$

THD is compensated for spectral leakage and noise.

12.11 TVE calculation

TVE is calculated by CPCM, for details see [10].

12.12 ROCOF calculation

ROCOF is calculated by CPCM, for details see [10], or by Andrew Roscoe's software, see [4].

13 References

[1] IEEE Std C37.118.1-2011, *IEEE Standard for Synchrophasor Measurements for Power Systems,* IEEE, 2011.

[2] A.J. Roscoe, S.M. Blair, B. Dickerson and G. Rietveld, “Dealing with Front-End White Noise on Differentiated Measurements Such as Frequency and ROCOF in Power Systems”, IEEE Transactions on Instrumentation and Measurement, Pages 1 to 13, April 2018.

[3] B. Dickerson, "Effect of PMU Analog Input Section Performance on Frequency and ROCOF Estimation Error," in IEEE AMPS (Applied Measurements for Power Systems), Aachen, 2015, p. 6.

[4] A. J. Roscoe, I. F. Abdulhadi and G. M. Burt, “P and M Class Phasor Measurement Unit Algorithms Using Adaptive Cascaded Filters”, IEEE Transactions on Power Delivery, Volume: 28 Issue: 3, 2013.

[5] X. D. Zhao, D. M. Laverty, A. McKernan, D. J. Morrow, K. McLaughlin, et al., "GPS-Disciplined Analog-to-Digital Converter for Phasor Measurement Applications," IEEE Transactions on Instrumentation and Measurement, vol. 66, pp. 2349-2357, Sep 2017.

[6] https://wiki.openelectrical.org/index.php?title=Symmetrical_Components

[7] Decimation (signal processing), available on line at:

https://en.wikipedia.org/wiki/Decimation_(signal_processing), Accessed 21/05/18.

[8] G. Crotti, D. Giordano, D. Bartalesi, C. Cherbaucich, and P. Mazza, “Set-up of calibration systems for inductive and electronic measurement transformers”, in Applied Measurements for Power Systems (AMPS), 2013 IEEE International Workshop on, Sep. 2013, pp. 24–28. doi: 10.1109/AMPS.2013.6656220.

[9] J. Horska, S. Maslan, J. Streit, and M. Sira, “A validation of a THD measurement equipment with a 24-bit digitiser”, in 2014 Conference on Precision Electromagnetic Measurements (CPEM 2014), Aug. 2014, pp. 502–503. doi: 10.1109/CPEM. 2014.6898479.

[10] U. Pogliano, J.-P. Braun, B. Voljc, and R. Lapuh, “Software Platform for PMU Algorithm Testing”, IEEE Transactions on Instrumentation and Measurement,vol.62, no. 6, pp. 1400–1406, Jun. 2013, ISSN: 0018-9456, 1557-9662. doi: 10.1109/TIM. 2013.2239051. (accessed on 01/05/2016).

Document Control Page

Owner (Holds the master copy)

Name (Partner):	Paul Wright
Partner:	NPL
E-mail:	paul.wright@npl.co.uk

Context (owner to update)

Author(s) (Partner):	Paul Wright (NPL), Martin Sira (CMI), Andrew Roscoe (STRAT), Gert Rietveld (VSL)
WP/Task/Activity:	WP3 / T2/ A3.2.7

Document Status (owner to update)

DEADLINE:	May 2019
Version:	1.4
Last modified:	01 May 2019
Status:	Delivered